Marine Geology 380 (2016) 174–190

Contents lists available at ScienceDirect

Marine Geology

journal homepage: www.elsevier.com/locate/margo

Understanding the history of extreme wave events in the Tuamotu Archipelago of French Polynesia from large carbonate boulders on Makemo Atoll, with implications for future threats in the central South Pacific

A.Y. Annie Lau [a,b,*], James P. Terry [c], Alan D. Ziegler [a], Adam D. Switzer [d], Yingsin Lee [d], Samuel Etienne [e]

[a] Department of Geography, National University of Singapore, 1 Arts Link, Singapore 117570, Singapore
[b] School of Geography, Planning and Environmental Management, The University of Queensland, St Lucia Campus, Brisbane, Qld, 4072, Australia
[c] College of Sustainability Sciences and Humanities, Zayed University, P.O. Box 19282, Dubai, United Arab Emirates
[d] Earth Observatory of Singapore, Nanyang Technological University, 50 Nanyang Avenue, 639798, Singapore
[e] EPHE (École Pratique des Hautes Études), PSL Paris Research University, CNRS UMR 6554 LETG Dinard, France

ARTICLE INFO

Article history:
Received 22 December 2015
Received in revised form 14 April 2016
Accepted 21 April 2016
Available online 22 April 2016

Keywords:
Boulders
Waves
Tropical cyclone
Tsunami
Historical records
South Pacific

ABSTRACT

Numerous large carbonate boulders up to 164 tonnes in mass were investigated on the reef flat and beaches of Makemo Atoll in the Tuamotu Archipelago of French Polynesia to reveal the past occurrence and to anticipate the future potential threat of extreme wave events, possibly generated by tropical cyclones and tsunamis. The modern reef edge and emerged mid-Holocene coastal landforms were identified as sources of boulders mobilized during extreme wave events in the past. The minimum flow velocities produced by extreme wave events were estimated to exceed 5.4–15.7 m/s at the reef edge on different parts of the atoll. Comparison of uranium–thorium ages of boulder coral fabric with written historical records indicates that two large boulders (77 and 68 tonnes) were possibly emplaced on the reef flat by a powerful cyclone in February 1878. Although most boulder dates are older than the earliest historical cyclone and tsunami records in French Polynesia, their ages concur with the following: (a) periods of "storminess" (i.e. increased cyclone activity compared to today) in the central South Pacific over the last millennium; and (b) periods of high sea-surface temperature (SST) at the Great Barrier Reef, possibly associated with higher-than-normal SSTs Pacific-wide that facilitated the generation of cyclones affecting the central South Pacific Ocean. None of the boulders on Makemo were dated younger than CE1900, implying that the last century has not experienced extreme waves of similar magnitude in the past. Nevertheless, the findings suggest that waves of comparable magnitudes to those that have transported large boulders on Makemo may recur in the Tuamotus and threaten island coasts across the central South Pacific in the future.

1. Introduction

The Tuamotu Archipelago (Tuamotus) consists of 77 atolls and one emerged limestone island, spread over 1500 km in a WNW-ESE chain across the central South Pacific Ocean. Extreme wave hazard assessment on these inhabited islands is hindered by the short and potentially incomplete historical record of tropical cyclones and tsunamis in the region, as well as the infrequent occurrence of such events in modern times. Proxy information is therefore useful for assessing the current-day threat. However, fine-grained sedimentary evidence, such as tsunami- or cyclone-deposited sand sheets, is not readily preserved in beach stratigraphies on low-lying coral atolls because of continual reworking by waves (Paris et al., 2010). Narrow atoll rims are also not ideal locations for the preservation of storm ridges of reef-derived gravel. Consequently, larger deposits, in particular tall-standing carbonate boulders that originate from the reef framework, are important features for investigating the age of, and energy associated with, extreme wave events in the archipelago. Such research has proven effective on the Great Barrier Reef of Australia (Nott, 1997; Yu et al., 2012; Liu et al., 2014), the Ryukyu Islands of Japan (Suzuki et al., 2008; Goto et al., 2010; Araoka et al., 2013), Tongatapu Island in Tonga (Frohlich et al., 2009); Sumatra in Indonesia (Paris et al., 2010); Taveuni Island in Fiji (Etienne and Terry, 2012); Bonaire in the Caribbean (Engel and May, 2012) and Lanyu Island in Taiwan (Nakamura et al., 2014).

The overall aim of this research is to improve current understanding on the potential threats of extreme marine wave hazards, namely tsunamis and tropical cyclones, for the atolls of the central South Pacific region. This is achieved by examining the extreme wave event history for the Tuamotus of French Polynesia. The objectives are threefold. First, the physical characteristics of the atolls in the Tuamotus and their relationship with Holocene sea-level change in the central South Pacific are

* Corresponding author.
E-mail address: annie.lau@uq.edu.au (A.Y.A. Lau).

http://dx.doi.org/10.1016/j.margeo.2016.04.018
0025-3227/

examined (Section 2). Second, a comprehensive record of historical tsunamis and tropical cyclones is compiled for the Tuamotu Archipelago (Section 3). Third, field investigation of numerous large carbonate boulders on the reef flat of Makemo Atoll in the archipelago is conducted to interpret how and when boulders were transported (Sections 4 and 5). Finally, these findings are compared with the historical records of tsunamis and cyclones in attempt to assess the threat associated with extreme wave events in the greater Tuamotus.

2. Study area

2.1. The Tuamotu Archipelago

The Tuamotu Archipelago (Fig. 1) is one of the five island archipelagos of French Polynesia; the others are the Society, Austral, Marquesas and Gambier archipelagos. Situated far from any tectonic boundary, the atolls in the Tuamotus were built on top of volcanic basements that formed from hot spot activity at least 37.5 million years ago (Clague and Jarrard, 1973; Pirazzoli et al., 1988a). The submarine volcanic edifices supporting the archipelago rise over 4000 m from the ocean bottom at an angle exceeding 45°. Submarine slopes become more gradual at a depth of 1000 m (Vitousek, 1963; Jordahl et al., 2004). At the sea surface, low-lying islands form on top of atoll reefs. They are composed of coral rubble deposited by waves on the old coral platforms. The elevation of these coral islands rarely exceeds 10 m above sea level (Dupon, 1986; Etienne, 2012).

Annual weather in the Tuamotu Archipelago varies little. Humidity is high (~80%) most of the time; the summer season has a slightly higher temperature from November to April (25–30 °C) than the other six-month period (24–28 °C) (Sachet, 1983). The Tuamotu coasts are microtidal, with tides ranging from 0.2 to 0.7 m. Most waves are 1–3 m high and break at periods of 6–9 s (Intes and Caillart, 1994). The yearly average wave height measured in the western Tuamotus is 1.6 m (Andréfouët et al., 2012), although prevailing north-east trade winds can reach 30 knots and generate swells of 3–5 m in amplitude. As a result, islands of coral shingle have formed on the north-eastern atoll rims over time (D'Hauteserre, 1978; Pirazzoli and Montaggioni, 1988).

2.2. Holocene sea-level change and tectonics in the Tuamotu Archipelago: influence on coastal geomorphology

Relative sea-level change during the last glacial maximum (LGM) (23,000–17,000 BP) in the Tuamotu Archipelago was measured from the coral reef record at Mururoa Atoll at approximately 135–143 m below present sea level (p.s.l.) (Camoin et al., 2001). Following the post-LGM marine transgression, the sea level was estimated at 17–23 m below p.s.l. at 9000 BP, then rose sharply to 2–3 m below p.s.l. at about 8000 BP (Camoin et al., 2001). Sea level in the Tuamotus reached a Holocene highstand of 0.8 ± 0.2 m above p.s.l. from about 4500 BP to after 2000 BP, but has since gradually dropped to present sea level (Pirazzoli and Montaggioni, 1988; Pirazzoli et al., 1988a). Alternatively, recent research has suggested the sea level highstand in the Tuamotus reached about 1 m above p.s.l. and remained stable until CE800, before dropping steadily until CE1900, then subsequently rose to present sea level during the last century (Dickinson, 2003).

Meanwhile, local tectonic activity has induced vertical movement of atolls. In the tectonically stable part of the archipelago towards Vahitahi and Mururoa at the eastern end of the atoll chain, thermal subsidence occurs (Pirazzoli et al., 1987a). The rate of subsidence of Mururoa is estimated at 7–8 mm/1000 years, as determined by the K-Ar dating of the volcanic basement (Trichet et al., 1984; Camoin et al., 2001). In contrast, tectonic uplift is evident at the southern boundary on Makatea and Anaa (raised coral atolls), owing to lithospheric flexure associated with the hotspot where Mehetia is currently located and which created Tahiti during the Pleistocene (Montaggioni et al., 1985; Pirazzoli et al., 1988b; Pirazzoli and Montaggioni, 1988; Montaggioni and Camoin, 1997; Dickinson, 2001) (refer to Fig. 1).

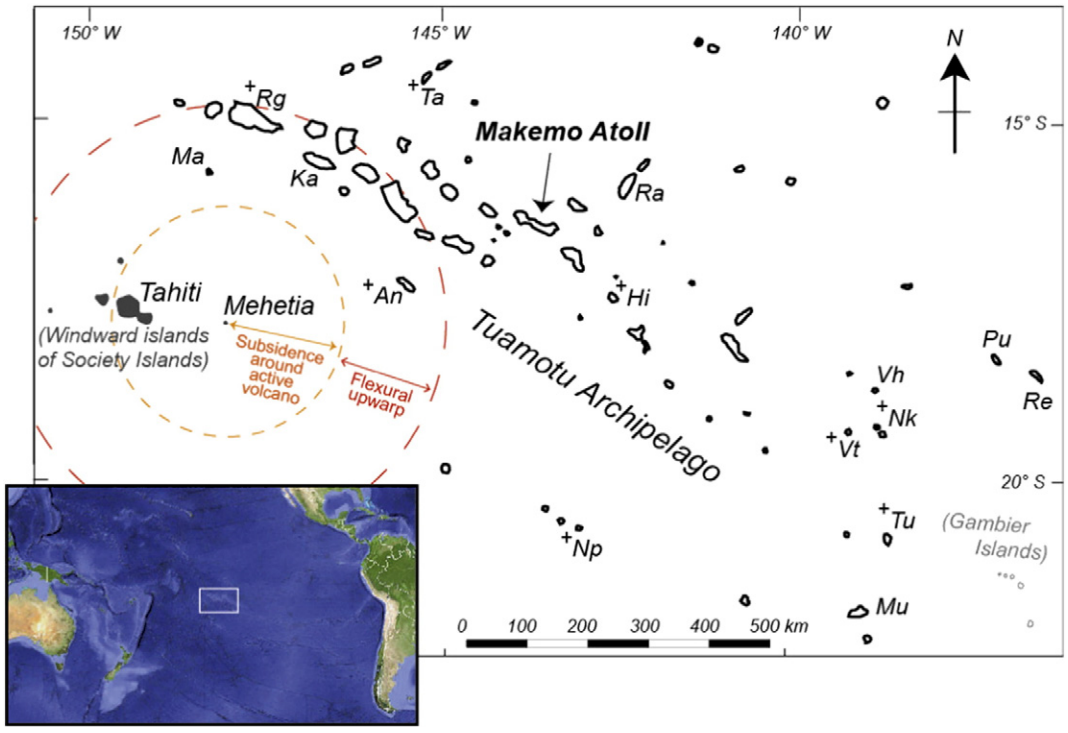

Fig. 1. Location map of Makemo Atoll in the Tuamotu Archipelago of French Polynesia. The hotspot that created Tahiti in the Pleistocene is currently located at Mehetia. This active volcano is causing subsidence around Mehetia, and the emergence of atolls including Anaa and Makatea due to flexural upwarp (red circle) outside the cone of subsidence (orange circle). Inferred extent of tectonic vertical movements is adapted from Dickinson (2001). Locations of other atolls mentioned in the text are also labelled. A "+" indicates that large boulder deposits have been reported by others (see Section 3.3). +An = Anaa; +Hi = Hikueru; Ka = Kaukura; Ma = Makatea; Mu = Mururoa; +Nk = Nukutavake; +Np = Nukutepipi; Pu = Pukarua; Ra = Raroia; Re = Reao; +Rg = Rangiroa; +Ta = Takapoto; +Tu = Tureia; Vh = Vahitahi; +Vt = Vairaatea. (Inset from Google Map).

The combined effects of late Holocene sea-level fall and local tectonic influences have resulted in the slight emergence of mid-Holocene reefs above modern sea level on atolls across the Tuamotu Archipelago. Emerged mid-Holocene reefs are generally found at elevations ranging from 0.8–1.1 m. On the most uplifted atoll, Anaa, Holocene coral reefs (^{14}C age 2000–2600 BP) occur at 1.3–1.5 m above p.s.l. (Montaggioni and Camoin, 1997; Dickinson, 2001). Emerged Pleistocene reefs and deposits are also preserved as evidence of tectonic uplift and local sea-level fall on Tuamotu atolls. Examples include emerged reefs 4–5 m high on Anaa and up to 3.5 m on Kaukura (Pirazzoli and Montaggioni, 1986; Pirazzoli et al., 1988b). Elevated dome-shaped remnants of Holocene algal crusts, indicators of past sea level, are also present on some atolls. Exfoliation of emerged reef flats, coral conglomerate platforms, and coralline algal crusts by mechanical erosion, mostly during cyclonic events, have also been observed on several southern atolls: Rangiroa, Reao, Vahitahi and Pukarua (Stoddart, 1969; Ricard, 1985; Pirazzoli et al., 1987a, 1987b, 1988a).

2.3. Makemo Atoll

Makemo Atoll (16°37′S, 143°40′W), lying in the middle region of the Tuamotu Archipelago, is the fourth largest atoll in the group (~670 km^2). The atoll is oriented NW-SE and has a length of 65 km (Fig. 2). The leeward reefs in the south of the atoll are mostly submerged. The windward reefs in the north of the atoll have low islands with vegetation covering 56 km^2. The islands support one village, Pouheva, having a population of less than 900 (L'Institut de la statistique de la Polynésie française, 2012).

On the northern shore, two deep passes (*ava* in Polynesian) connect the lagoon with the open ocean and separate the low-lying coral islands (Fig. 2). Carbonate boulders are found mainly on the 70–100 m wide reef flat that is expanding by accretion in an oceanward direction to the north. A red algal reef crest comprising *Porolithon* or *Lithothamnion* (primary reef-building algae types) occurs at the reef edge where wave energy is highest. Emerged features, including Holocene reefs, coral conglomerate platforms, and beachrock are exposed at heights of no more than 0.6 m on and behind the modern reef flat on some parts of the shore (Fig. 3). A narrow beach up to 20 m wide, composed primarily of coral debris of sand to cobble size, is located further behind.

Three to four zones of corals can be identified on the submarine reef slope on Tuamotu Atoll reefs (Bruckner, 2014). The uppermost 5–10 m consists mainly of the short branching corals *Acropora* and *Pocillopora*. A mixed zone of branching, encrusting and massive corals are found at 10–15 m depths. A dominance of domal and platy corals, including *Porites*, *Montipora* and *Astreopora*, extend to 15–20 m. Encrusting corals and elephant skin corals *Pachyseris* can be found below 20 m, reaching depths over 40 m in some cases (Bruckner, 2014).

3. Historical extreme wave events in the Tuamotus

3.1. Tropical cyclones and storms

The cyclone season in the South Pacific commonly extends from November to April. On average, about nine tropical cyclones occur east of the 160°E meridian each year; however, the number per year was found to vary greatly from 3 to 17 during the period 1970 to 2006 (Terry, 2007). This annual variability is largely related to the El Niño Southern Oscillation (ENSO). More tropical cyclones and typically stronger storms occur in the central South Pacific in El Niño years (Revell and Goulter, 1986; Terry and Gienko, 2010). The eastward shift of warmer SSTs during El Niño years also allows more storms to travel further east into the central South Pacific where the Tuamotus are located.

Tropical cyclones are not frequent within French Polynesia (Larrue and Chiron, 2010). Cyclone hazard assessments suggest a 50-year return period for waves exceeding 12 m at both the Tuamotus and Tahiti in the Society Islands (Météo-France, 1995; Damlamian et al., 2013; Stephens and Ramsay, 2014). DeAngelis (1983) stated that only 20 tropical cyclones affected the Tuamotus in the 150 years extending from 1825 to 1982 (cited by Ruminski, 1990). However, in the cyclone season of 1982–83, a period under the strong influence of an El Niño event that caused the sea surface near the Tuamotus to be significantly warmer than normal years, five tropical cyclones and one tropical depression occurred in the duration of six months. Five of these storms tracked passed the Tuamotus, causing sea flooding to a depth of more than 1 m, soil erosion, and displacement of coral rubble on the atolls (Dupon, 1986; Etienne, 2012).

In total, approximately only 24 known (including some doubtful) tropical cyclones have affected the Tuamotus in 192 years spanning 1822–2014 (Table 1). The record of storm history is fragmented, as exemplified by the fact that only one storm in 1958 was documented for the 72 years between 1907 and 1979. Sachet (1983) commented that

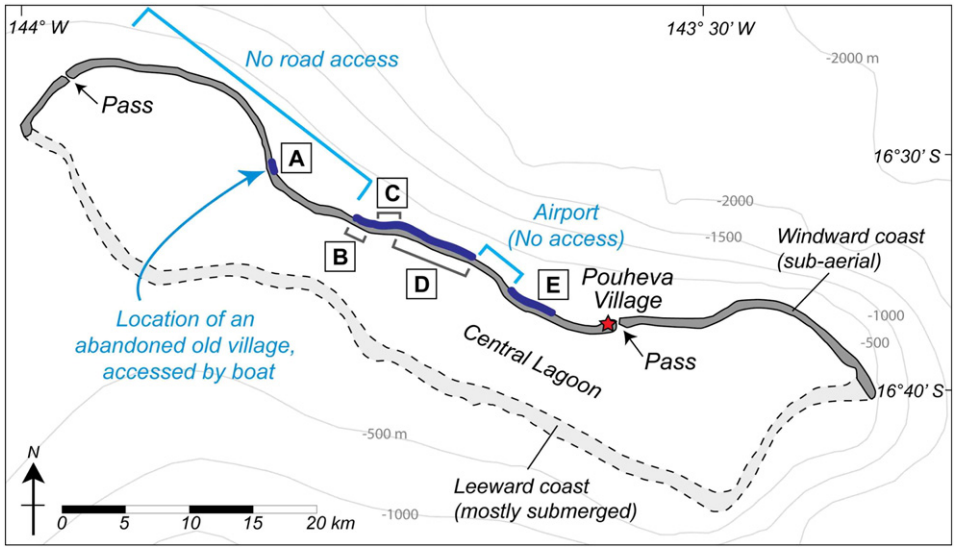

Fig. 2. Makemo Atoll in the central Tuamotu Archipelago consists of windward low islands forming the north coast (dark grey shading), submerged leeward reefs in the south (light grey), a central lagoon (white area between the reefs). There are two deep passes connecting the central atoll lagoon to the open Pacific. Parts of the shore (blue shading) were visited for boulder data collection, and these shores were divided into five zones (A to E) for analyses.

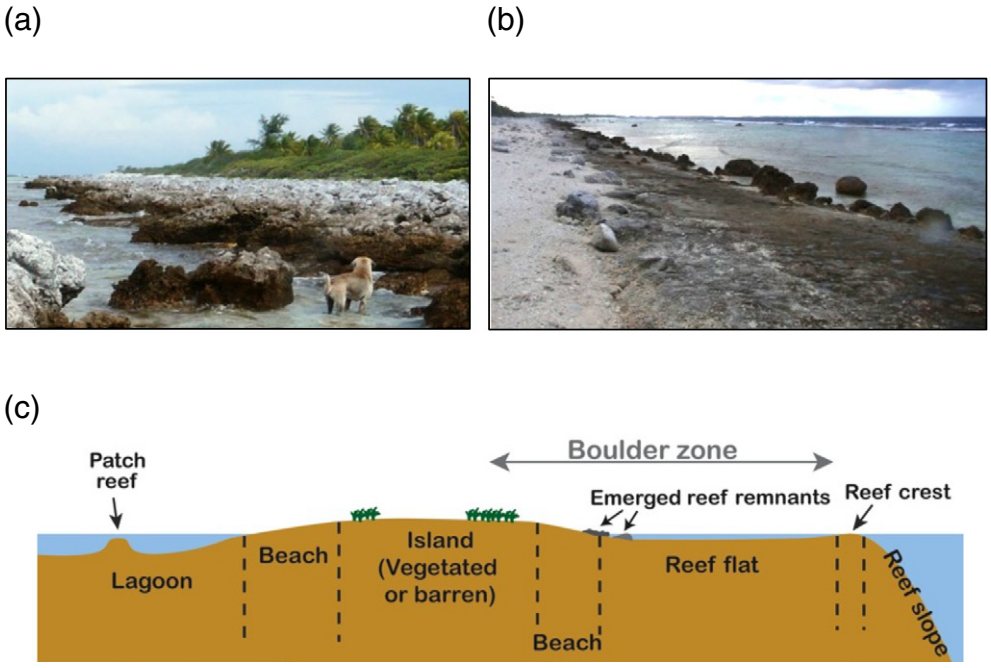

Fig. 3. Emerged coastal features including (a) emerged reef remnants of different forms and (b) calcareous beachrock are present at parts of the northern rim. (c) A generalized profile and zonations of the Makemo windward island. Algal reef crest is formed on the reef edge where wave energy is the highest, which is the source of most wave-transported boulders. Boulders are mostly deposited on the 70–100 m reef flat, while some were transported farther onto or behind the beach. Diagram is not drawn to scale.

there must have been other storms in pre-European times, but there is no written record verifying this.

The cyclones in the unusual 1982–83 season, and the damage they brought to the Tuamotus, have been reported in great detail (e.g. Harmelin-Vivien and Stoddart, 1985; Dupon, 1986). Storm surges 3–4 m in height and flooding of inhabited areas to more than 1 m were experienced on some atolls (Harmelin-Vivien and Stoddart, 1985; Dupon, 1986). Very high waves were reported by eyewitnesses on Tureia (16–18 m), Hao (15 m) and Anaa (12 m) (des Garets, 2005; Damlamian et al., 2013). As a result of powerful surges and waves, large boulders excavated from beachrock and reef slopes were thrown onto the reef flats, in boulder ramparts, across the inter-island passages (*hoa* in Polynesian), or into atoll lagoons (Sachet, 1983; Harmelin-Vivien and Stoddart, 1985). Sheets of coral shingle and rubble were also deposited on shorelines, while both accumulation and erosion of sand on small islets and in channels were noticed on different parts of the affected atolls (Sachet, 1983; Dupon, 1986). It is more difficult to assess the impacts of older cyclones but interesting perspectives emerge with multidisciplinary approaches. Correlating cyclone velocity and atmospheric pressure derived from various archives, Canavesio (2014) suggested that waves as high as 15.5–18.5 m might have swept Anaa Atoll during the February 1906 cyclone that killed between 95 and 130 inhabitants.

Cyclone-generated swells are a common hazard in French Polynesia (Canavesio, 2014). These swells are usually generated by cyclone systems outside of the territory, most often coming from the western Pacific (Etienne, 2012). In the Tuamotu Archipelago, swell amplitudes of up to 10–15 m were recorded during the 1982–1983 cyclone season. The mean cyclonic swell height normally ranges between 4 and 12 m (Ministère du Développement Durable, 2006 as cited in Etienne, 2012). As cyclonic swell hazard is not documented systemically in the region, the return period for large swells cannot be determined. Yet it can be assumed that strong cyclones tracking through or near the Tuamotus likely generated high swells, affecting the atolls. Cyclonic swells can also travel long distances. For instance, Cyclone Pam in March 2015 caused much destruction as it tracked through the southern islands of Vanuatu. But its powerful swells also damaged infrastructure on Tarawa Atoll in Kiribati, more than 1000 km distant to the north east (Stone, 2015). This example indicates how Makemo might be affected by swells from cyclones that track anywhere within the French Polynesian territory.

3.2. Tsunamis

The historical tsunami record is very limited in the Tuamotu Archipelago (Etienne, 2012). It has been suggested that due to the steep submarine slope and small size of atoll islands, relative to long tsunami wavelengths, amplification of waves upon shoaling is minimal, resulting in little destruction by tsunami waves on atolls (Vitousek, 1963; Stoddart and Walsh, 1992; Reymond et al., 2012). However, the impact of the 2004 Indian Ocean Tsunami in the Maldives has shown that atolls are not immune to the destructive forces of tsunami waves. In 2004, wave heights of 1.8 m together with extensive flooding caused damage of infrastructure on Malé Island at southern North Malé Atoll. More than 80 lives were lost in the Maldives during the 2004 Indian Ocean Tsunami (Kench et al., 2006, 2008).

Nevertheless, both numerical modelling and recent observations during tsunamis have demonstrated that the Tuamotu atolls, being protected by fringing reefs, receive smaller tsunami waves and sustain less damage than volcanic islands in other archipelagos of French Polynesia (Sladen et al., 2007). According to written records, changes in water level were observed in the Tuamotus followed the generation of tsunamis occurring in 1946 (Aleutian Island earthquake), 1960 (Chile earthquake), 2009 (South Pacific earthquake), 2010 (Chile earthquake) and 2011 (Tohoku-oki earthquake in Japan). Yet, Tuamotu atolls suffered only moderately in the 1946 and 1960 events (Reymond et al., 2012). Islanders observed water level changes of less than 1 m on several inhabited atolls during the 1960 Chile tsunami (Vitousek, 1963). Whereas in the Marquesas Archipelago, where volcanic islands are not protected by coral reefs, run-ups exceeding 10 m followed the 1946 and 1960 tsunamis (Schindelé et al., 2006; Etienne, 2012).

An oral tradition of a plausible tsunami dating from the 16th century was reported by Bourrouilh-Le Jan and Talandier (1985) citing Ottino

Table 1
Details of historical cyclones tracked through and affected the Tuamotus since 1822.

Date (Name of storm)	Cyclone season/El Niño intensity (if any)	Damage/descriptions	Ref. #
1822	Unknown	Anaa and neighbouring atolls devastated	6
1825	Unknown	Anaa hit by storm	6
21 Jan. 1856 (Recorded in the Society Islands)	1855–56	HMS Dido of British Royal Navy was dismasted in a cyclone off Raiatea of the Society Islands.	4
Jan 1877	1876–77 No El Niño	"*Several storms caused damage to various atolls including Manihi*" (Sachet, 1983, p.3)	2,6
Sept 1877	1877–78 Strong El Niño	Hurricane of particular force "*Several storms caused damage to various atolls including Manihi*" (Sachet, 1983, p.3)	1,2,5,6
6–7 Feb. 1878		Hurricane of particular force Extremely violent, 117 people killed in Kaukura. Damage done by storm tides rather than wind.	1,2,5,6,7
14–15 Jan. 1903	1902–03 Moderate El Niño	Hurricane of particular force Devastated a large number of atolls, 515 people died including 377 on Hikueru Atoll. Damage done by storm tides rather than wind. Boulders of 4–5 t or/and 4–6 m in length deposited on Raroia	2,4,6,7
23–25 Mar. 1905	1904–05 Moderate El Niño	Extensive damage on Manihi and Takaroa	2,6,7
6–8 Feb. 1906	1906–07 Moderate El Niño	Hurricane of particular force Immense damage in the Society Islands and Tuamotus, including on Manihi and Takaroa atolls. North coasts flooded, at least 121 people killed. Damage caused by storm tides rather than wind. Boulders 4–6 m in length deposited on Rangiroa	2,5,6,7
Jan. 1958 (Doubtful event)	1957–58 Strong El Niño	"*Teissier (1969) mentions only one more storm to hit the Tuamotus, in Jan. 1958*" (Sachet, 1983, p.4) But according to Ref # (9), no cyclone tracked through or near to the Tuamotus in this cyclone season.	3,6,12
5–9 Dec. 1977 (Tessa)	1977–78 Weak El Niño	Tracked at north of the Tuamotus with a minimum pressure of 990 hPa	3,11
27–29 Nov. 1980 (Diola)	1980–81 No El Niño	Originated and travelled in the Tuamotus, max wind speed 35 knots	3,6,13
22–26 Jan. 1983 (Nano)	1982–83 Strong El Niño	Originated and travelled in the eastern Tuamotus	3,6,7
22–27 Feb. 1983 (Nisha/Orama)		Passed close to Takapoto-Manihi area, demolishing buildings and installations, breaking tress, piling up coral shingle, tearing up large blocks of coral from reef and throwing them on reef flats	3,6,7
6–14 Mar. 1983 (Rewa)		Boulders transported on Nukutipipi (up to 30 m^3), Takapoto (unrecorded size), Anaa (45–145 m^3, by Cyclone Orama)	3,6,7
7–13 Apr. 1983 (Veena)			3,6,7
17–21 Apr. 1983 (Williams)		Originated and travelled in the eastern Tuamotus.	3,6,7
5–17 Dec. 1991 (Wasa/Arthur)	1991–92 Strong El Niño	Maximum mean winds 45 m/s, lowest pressure 976 hPa. Tracked passed the southern Tuamotus near Mururoa, but most damage was in the Society Islands where properties were destroyed.	8
5–9 Feb. 1992 (Cliff)		Originated at north of the Tuamotus and travelled through eastern Tuamotus. No damage record found.	3,12
29 Jan.- 2 Feb. 1998 (Ursula)	1997–98 Strong El Niño	Passed through the Tuamotus, damage done by pre-cyclone swell rather than winds.	3,8
30 Jan.- 3 Feb. 1998 (Veli)		Passed through the middle of the Tuamotus. TCs Ursula and Veli together damaged houses, roads and bridges on Mataiva, and a few houses on Makatea. Airstrip on Rangiroa disrupted by coral and sand washed up. No loss of life in these two events.	3,9
29 Apr.- 3 May 1998 (Bart)		Weak cyclone (tropical depression) passed over the Tuamotus. Ten people killed when waves capsized a boat.	3,9
23–29 Feb. 2000 (Kim) (Cyclone did not track through the Tuamotus)	1999–2000 No El Niño (Strong La Niña)	Tracked south of the Tuamotus. Swells exceeded 2 m were recorded at the Gambier Islands in southeast of the Tuamotus.	3,10,12
29 Jan.- 8 Feb. 2010 (Oli) (Cyclone did not track through the Tuamotus)	2009–10 Strong El Niño	Did not track in the Tuamotus but as a severe tropical cyclone of category 4, much damage was done on the Society Islands and the Austral Archipelago by the storm and related large swells. According to a resident on Makemo Atoll, the low-lying beach was flooded during the storm.	3,12

References:
For El Niño condition identification
1: Allan and Nicholls (1991).
2: Wolter and Timlin (2011).
3: NOAA Climatic Prediction Center (2015).
For cyclone descriptions
4: Editor of The Nautical Magazine (1856)
5: Stoddart (1969), quoted directly from Geographical handbooks Series (1943).
6: Sachet (1983), referred to the work of Morenhout (1937), Giovanelli (1940); Teissier (1969) and DeAngelis (1983).
7: Bourrouilh-Le Jan and Talandier (1985), using data from Meteorological Bureau of Papeete, Tahiti, French Polynesia.
8: Gill (1994).
9: Chappel and Bate (2000).
10: Tahitipress (2010).
11: Southern Hemisphere Tropical Cyclone Data Portal (2011).
12: Joint Typhoon Warning Center Tropical Cyclone Best Track Data Site (2014).
13: NOAA national climatic data center (2014).

(1965) from Rangiroa Atoll in the eastern Tuamotus. The folklore refers to the conditions related to a sudden and brutal catastrophe that destroyed the western and south-western of Rangiroa. A passage begins "*Sous le soleil mettant des éclairs éblouissants dans le creux des immenses vagues*" (Bourrouilh-Le Jan and Talandier, 1985, p. 314), which translates to "Under the setting sun, dazzling flashes in the troughs of huge waves". Sunny weather mentioned simultaneously with huge waves implies the event was a tsunami rather than a cyclone.

Tsunamis believed to have affected other parts of French Polynesia may have also struck the Tuamotu atolls. Bourrouilh-Le Jan and Talandier (1985), for example, have inferred the possible occurrence of multiple tsunamis in the Marquesas Archipelago from the abandonment of coastal habitats. Similarly, examining archaeological and geomorphological features in various Pacific Island countries, Goff et al. (2011) presented the case for four plausible palaeo-tsunamis that could have affected French Polynesia. Three abandoned occupation sites preserved under sand layers on Ua Huka, Nuka Hiva and Rurutu islands might have resulted from a single tsunami generated by the 1450 earthquake, which Goff et al. (2012) proposed occurred at the Tonga-Kermadec Trench (TKT), 3000 km west of the Tuamotus. A summary of these "equivocal" events is presented together with other historical tsunamis reported in the Tuamotus in Table 2.

3.3. Wave-deposited boulders on Tuamotu atolls: published accounts

Owing to the low relief of atolls in the Tuamotus, large blocks and boulders are prominent features that have been recorded historically. In the eastern Tuamotus, a giant reef boulder (approx. 150 m^3) on Vairaatea was indicated on the French chart no. 5878 as a "Rocher Noir" or black rock (Pirazzoli et al., 1988a). Two other reef boulders of up to 15 m^3 were found on Nukutavake Atoll; and several boulders of up to 30 m^3 were found on Tureia. All of these boulders were considered in earlier publications to be remnants of past cyclones (Pirazzoli et al., 1988a). Carbon-14 dating of boulder coral fabric suggests that the wave events that brought them on land spanned the period 3995–1220 BP (Pirazzoli et al., 1988a).

One prominent reef boulder dated at 1470 ± 60 BP exists on Hikueru in middle of the Tuamotu Archipelago (Pirazzoli et al., 1988a). As it is situated on top of a pedestal that is 0.7 m above the present reef flat, this boulder is believed to have been emplaced onto the reef by cyclonic waves when the sea level was higher (Pirazzoli et al., 1988a). Meanwhile on Raroia, boulders weighing 4–5 t were transported onto the coast by a cyclone in 1903 (Giovanelli, 1940). Boulders on Nukutipipi Atoll up to 30 m^3 in size were emplaced by one of the tropical cyclones during the unusual 1982–83 cyclone season (Salvat and Salvat, 1992).

Table 2
Details of confirmed historical tsunamis and possible/inferred palaeo-tsunamis in the Tuamotus or French Polynesia in general.

Date /period	Location affected	Tsunami source	Evidence	Impact/remarks	Ref. #
Confirmed historical tsunamis in the Tuamotu Archipelago					
1 Apr. 1946	The Tuamotus	Earthquake (Mw = 8.1) in the Aleutian Islands, Alaska	Witnesses report	Wave height 1.9 m at Hao atoll	6
22 May 1960	The Tuamotus	Earthquake (Mw = 9.5) at Chile	Witnesses report	Observation of water-level changes of <1 m reported from multiple atolls	1
29 Sept. 2009	The Tuamotus	Earthquake (Mw = 8.2) in the Samoa Islands, South Pacific	Tide gauge record	Wave height 0.4 m at Rangiroa atoll	7
27 Feb. 2010	The Tuamotus	Earthquake (Mw = 8.8) at Chile	Tide gauge record	Wave height 0.3 m at Rikitea Island	8
11 Mar. 2011	The Tuamotus	Earthquake (Mw = 8.9) at east Japan	Tide gauge record	Wave height 0.29 m at Rangiroa	9
Possible tsunami at the Tuamotu Archipelago					
16th century	Rangiroa, the Tuamotus		Oral tradition	Sudden and brutal waves, destroyed settlements in SW and S Rangiroa	2
Inferred tsunami affecting other parts of French Polynesia					
Late first millennium	Hane of Ua Huka, the Marquesas		Sudden abandonment of coastal habitats	Inferred from ethnology studies	3
CE1430–1570	Ua Huka, the Marquesas	Possibly an earthquake in South America. (or possibly the 1450 TKT Tsunami)	Mobilised coastal dune covering occupation	Date inferred from carbon-14 dating of soil and skeletons.	10
CE1450–1500	Nuka Hiva, the Marquesas	Possibly from the 1450 TKT Tsunami	Clean sand sheet between archaeological layers	The sandsheet could be deposited from a major storm. Date inferred from carbon-14 dating of archaeological units.	10
CE1450–1600	Rurutu, the Australs	Earthquake at Tonga Trench or South America (Possibly the 1450 TKT Tsunami)	Clean sand sheet between archaeological layers	Date inferred from carbon-14 dating of cultural units.	10
16th century	Hane of Ua Huka, the Marquesas		Sudden abandonment of coastal habitats	Inferred from ethnological studies	3
Possibly 16th century	Huahine, Raiatea and Scilly, Society Islands		Sudden abandonment of coastal habitats	Inferred from ethnological studies	4,5
Post 1650	Huahine, Society Islands		Clean sand layer on top of abandoned occupation	Date inferred from carbon-14 dating of bone underneath sand layer.	10

References:
1: Vitousek (1963).
2: Ottino (1965) as cited in #7.
3: Kellum Ottino (1971) as cited in #7.
4: Sinoto (1978) as cited in #7.
5: Semah (1979) as cited in #7.
6: Bourrouilh-Le Jan and Talandier (1985).
7: CEA (2009).
8: CEA (2010).
9: Pacific Tsunami Warning Center (2011).
10: Goff et al. (2011).

Further west in the Tuamotus, large carbonate boulders (of unrecorded size) on the northwest reef of Takapoto similarly originated from cyclones in 1982–83 (Sachet, 1983). On the western rim of Anaa Atoll, seven boulders (25–145 m^3) moved by Cyclone Orama on the reef flat in 1983 were measured by Etienne et al. (2014). Another eight larger boulders ranging in volume 150 to 450 m^3 were encountered, but causes of deposition are still unknown (Etienne et al., 2014). On Rangiroa, the largest atoll in the Tuamotus, large coral blocks can be found at multiple locations. Surveying three large blocks at the southern, western and northern rims, Stoddart (1969) found that the largest block on the western rim measured 5.5 × 5.5 × 4.5 m. Research by Bourrouilh-Le Jan and Talandier (1985) recorded numerous boulders on western atoll rims, with the largest block (15 × 10 × 5 m) weighting 1500 t. Recently the dimension and mass of this boulder were adjusted to 14 × 8 × 4.5 m (approx. 504 m^3) and about 1000 t (Etienne et al., 2014). While the cause of the waves that brought the largest block onto the reef has not been determined, boulders 4–6 m in length are believed to have been transported by cyclonic waves on Raroia and Rangiroa in 1903 and 1906 respectively (Stoddart and Walsh, 1992).

4. Methods

4.1. Data collection

On Makemo Atoll, numerous large boulders exist on the northern atoll rim. These have not previously been studied. Boulders measured in this investigation were chosen based on their size and accessibility. At the western section of the island, where approximately 0.7 km of coastlines had abundant boulders but no road access, only large (intermediate axes >2 m) clasts were measured (zone A in Fig. 2). Elsewhere, large and medium-sized boulders were chosen: clasts with intermediate (b-) axes less than 1 m were generally not measured. However, seven boulders with b-axes <1 m were included, either because they were only slightly below the chosen size threshold, or were deposited far inland behind the beach (135–161 m) where their presence was assumed to be representative of the limit of strong wave inundation. For boulder orientation and wave direction analyses, the studied shoreline was divided into five zones (A–E) according to the shore orientation (refer to Fig. 2).

For each selected boulder, the following information was recorded: (1) the dimensions of three axes (termed a-, b-, c-axes for long, intermediate, and short axis respectively) measured by tape; (2) the orientation of the a-axis in degrees; (3) shape (rectangular, triangular, or ellipsoidal); (4) GPS location (*Mobile Mapper 10*; spatial accuracy ± 0.5 m); and (5) the distance from the algal crest reef edge (determined with a Laser Technology TruPulse 360B laser rangefinder; accuracy ± 1 m). In cases where the distance to the reef edge could not be measured, for example when obstructions were present, the distance was estimated from satellite images available on Google Earth (accuracy estimated at 2 m). For boulder orientation analysis, only elongated boulders with a significant long axis (a-axis >20% longer than b-axis) were considered, because square boulders do not have a representative long axis for this analysis.

Carbonate samples were chiselled from 24 boulders for age-dating and density determination. Among them, 22 were dead coral samples taken from the surface of boulders; the other two samples were dead giant clams that had anchored on separate boulders. Samples were generally collected from boulders with the largest volume or those located farthest from the reef edge where waves break. Their ages therefore possibly represent occurrences of the strongest extreme wave events affecting the atoll.

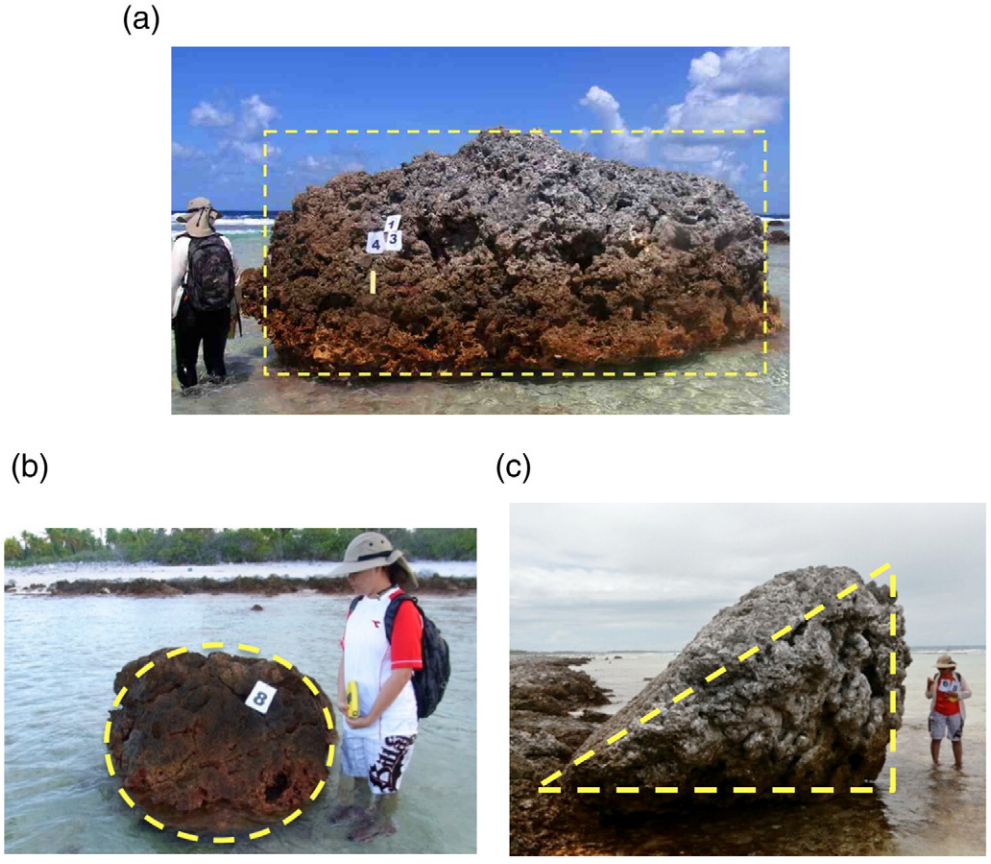

Fig. 4. Boulder volume was calculated based on general 3D geometric shapes. (a) As the simple geometric calculation of rectangular boulders results in significant overestimation of volume, their initial volumes were multiplied by a 0.7 scalar (see text). No correction was applied to (b) ellipsoidal or (c) triangular boulders.

4.2. Volume and density determination

The volume of each boulder was calculated based on its 3D geometric shape: e.g., rectangular prism ('rectangular'), triangular prism ('triangular'), or ellipsoidal. The volumes (V) were estimated thus:

Triangular boulders:

$$V = \frac{(a \cdot b \cdot c)}{2} \quad (1)$$

Ellipsoidal boulders:

$$V = \frac{4}{3}\pi\left(\frac{a}{2} \cdot \frac{b}{2} \cdot \frac{c}{2}\right) \quad (2)$$

Rectangular boulders:

$$V = 0.7\ (a \cdot b \cdot c) \quad (3)$$

where a, b, and c in all equations are the long, intermediate, and short axes. For rectangular boulders, volumes are almost always overestimated by the general geometric calculation $V = a \times b \times c$ because boulders are rarely perfectly rectangular (Terry et al., 2013). Comparison of accurate measurements of boulder volumes determined using terrestrial laser scanning, differential-GPS, and photogrammetric 3D modelling (Scicchitano et al., 2012; Engel and May, 2012; Gienko and Terry, 2014), has demonstrated that the actual volumes of boulders are only a fraction (0.41–0.76) of those estimated using rectangular geometry. Thus, in this study, 0.7 was used to minimize error in the estimation of boulder volume and mass (Eq. 3). A conservative value of 0.7 was used because observed boulders were not highly weathered into rugged, irregular shapes that would otherwise support the use of smaller scalars. No correction was needed for ellipsoidal and triangular boulders because their volumes are well approximated by simple geometric formulae (Fig. 4).

The bulk density (BD) of collected coral samples ($n = 22$) was used to calculate the mass (M) of all measured boulders ($M = BD \times V$) from estimated volumes. Spiske et al. (2008) highlighted that the porosity of boulders should not be neglected in density determination of wave-emplaced coastal boulders. They showed that Archimedean buoyancy measurements provide the most accurate estimation of coral density. Bulk density was therefore calculated based on the Archimedes principle:

$$BD = 1.02 \times \left[\frac{W_a}{(W_a - W_f)}\right] \quad (4)$$

where 1.02 g/cm^3 is the density of seawater; W_a is the dry weight (g) of sample in air; and W_f is the weight (g) of the sample in seawater. Dry weight was determined from 22 samples (17–83 g) with a digital balance (accuracy to 0.01 g). To measure the coral weight in seawater with a density of 1.02 g/cm^3, sea salt was added to a beaker of distilled water of known volume. Salinity was monitored with a calibrated, handheld salinity meter while stirring until the concentration reached that of natural seawater (35 ppt). The plastic-wrapped sample was then tied to a hanging scale and lowered into the beaker of seawater. The W_f value was measured immediately after sample submergence.

Bulk density was also be determined by a simple method using dry mass (M_a) and bulk volume (BV):

$$BD = M_a/BV \quad (5)$$

where M_a was determined in the same way as W_a above, and bulk volume of the same sample was determined via water displacement. Briefly, the plastic-wrapped sample was placed into a water-filled beaker and the difference in water level was recorded as the bulk volume of the coral sample.

4.3. Wave velocity estimation

Carbonate boulders on the Makemo reef flat originated from two plausible sources (Fig. 5): (1) the active reef edge or reef slope (collectively called "reef-edge boulders"); or (2) from mid-Holocene emerged

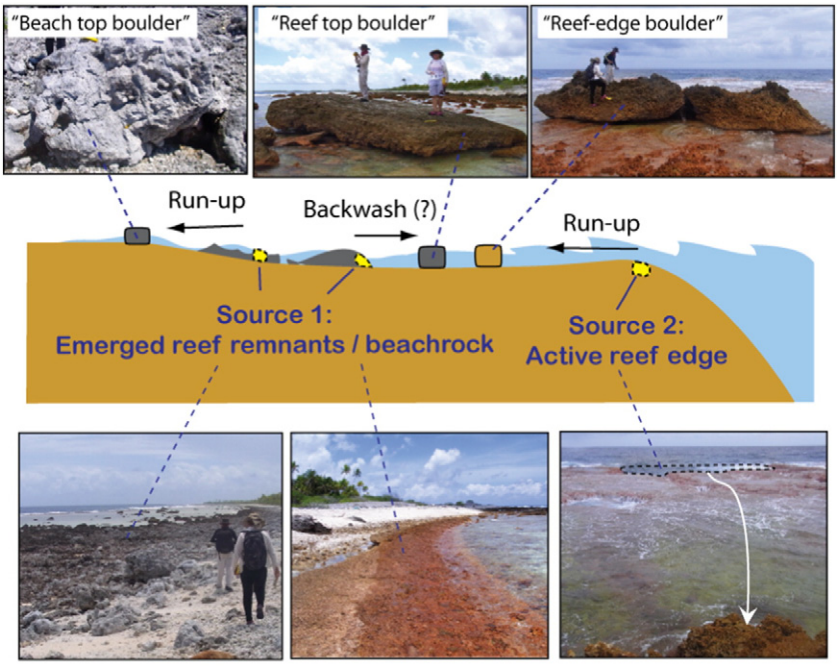

Fig. 5. Boulders on the coast of Makemo Atoll were derived from two possible sources: some originated from the emerged reef remnants or emerged beachrock (source 1) and were moved by either run-up waves (landward direction) or backwash (ocean direction). They were then deposited either behind the beach on the island as "beach top boulders", or on the reef surface as "reef top boulders". The surface appearance of these boulders is consistent with the local reef remnant; and the thickness of such boulders is within the range of reef emergence since the mid-Holocene. Most boulders in the dataset were however derived from the active reef (source 2) and referred to as "reef-edge boulders". At some parts of the reef edge, sockets of similar size as boulders deposited on reef flat were observed at the reef edge and could be identified as boulder sources.

reef remnants or other emerged features (collectively called "emerged reef boulders"). Reef-edge boulders were transported in the landward direction by run-up flow; while emerged reef boulders were transported either by run-up onto the beach in the landward direction, or by backwash to the reef flat in the ocean direction (Fig. 5). The direction of movement of the latter process is often debatable (discussed below in Section 5.1). When a boulder exhibited a surface appearance resembling that of the remnant reef at the locality, and had at least one axis that was shorter than the elevation of the emerged reef (approx. 1.1 m), the boulder was considered to originate from the emerged reef (i.e., "emerged reef boulders"). The emerged reef boulders were further divided into two groups based on their present location: "beach top" or "reef top" (Fig. 5).

The hydrodynamic flow transport equations proposed by Nandasena et al. (2011) were used for estimating plausible flow velocities that moved the carbonate boulders on Makemo. Assuming that clasts were already detached from the reef prior to transport, the minimum flow velocities (MFVs) required to initiate boulder transport from two different pre-transport positions by three initial transport modes were estimated (Nandasena et al., 2011). Boulders originally found occupying a non-obstructed surface (either subaerial (SA) or submerged (SM) setting) could be transported by sliding, rolling (overturning) or lifting because drag, inertia and lift forces can all be applied to the boulder by the flow to initiate movement. In contrast, for a clast resting in a joint-bounded (JB) socket, lift is the only force that can be applied initially, because only the top surface of the boulder is exposed, and lateral movement by sliding and rolling is restricted (Nandasena et al., 2011) (Fig. 6).

Emerged reef boulders located on the sub-aerial reef flat prior to movement could be transported by sliding, rolling or lifting (Fig. 6). Reef-edge boulders situated at elevations lower than the reef flat before movement, similar to the initial location for joint-bounded boulders, could only be transported onto the reef flat via lifting. After the boulder was lifted on to the reef flat, it could be moved further by sliding or rolling by lower flow velocities. According to Nandasena et al. (2011), the initial transport of a non-obstructed emerged reef boulder in a subaerial or submerged setting occurs for the following conditions via three processes:

$$u^2 \geq \frac{2\,(\rho_s/\rho_w - 1)gc(\mu_s\,cos\theta + sin\theta)}{C_d(c/b) + \mu_s C_l} \quad \text{(sliding)} \qquad \text{(n. 6)}$$

$$u^2 \geq \frac{2\,(\rho_s/\rho_w - 1)\,gc\,(cos\theta + (c/b)\,sin\theta)}{C_d\left(c^2/b^2\right) + C_l} \quad \text{(rolling)} \qquad (7)$$

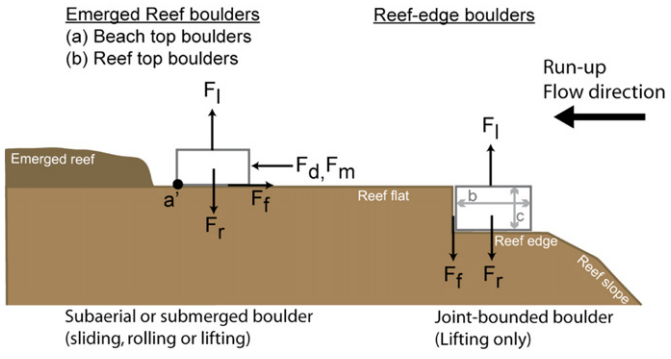

Fig. 6. Illustration of two different pre-transport settings (SA/SM on left; JB on right) and the respective possible transport modes (sliding, rolling and lifting). The boulder example on the left is an emerged reef boulder; the one on the right is a reef-edge boulder (see Fig. 5). The boulders are assumed to be rectangular, and detached from the bedrock with a-axis aligned normal to flow in the pre-transport position. F_d is drag; F_m, inertia; F_l, lift; F_f, friction; and F_r, restraining force. The variables b and c refer to the b- and c-axis, respectively. The term a' is the axis of overturning (rotation about the a-axis). The concept is adapted from Nandasena et al. (2011).

$$u^2 \geq \frac{2\,(\rho_s/\rho_w - 1)\,gc\,cos\theta}{C_l} \quad \text{(lifting)}. \qquad (8)$$

For a reef-edge boulder in a joint-bounded setting, transport can only be initiated by lifting when:

$$u^2 \geq \frac{2\,(\rho_s/\rho_w - 1)\,gc\,(cos\theta + \mu_s\,sin\theta)}{C_l}. \qquad (9)$$

In all equations, u is flow velocity (m/s); b and c are the b- and c- axes (m), respectively; ρ_s, boulder density; ρ_w, water density (1.02 g/ml); C_d, drag coefficient ($C_d = 1.95$); C_l, lift coefficient ($C_l = 0.178$); θ, angle of the bed slope at pre-transport location; μ_s, coefficient of static friction ($\mu_s = 0.5$); and g, acceleration of gravity ($g = 9.81\ m/s^2$).

Because the studied reef flat is not inclined, the angle of the bed slope θ is set at 0°. When $\theta = 0°$, the calculated flow velocity required to initiate boulder transport by lifting is the same for both non-obstructed (SA or SM; Eq. 8) and joint-bounded pre-transport conditions (Eq. 9), because sine $\theta° = 0$.

4.4. Coral age-dating

The ages of surface coral samples collected from 20 boulders were measured by uranium-thorium (U-Th) dating using high-precision thermal ionization mass spectrometry (TIMS) at the Radiogenic Isotope Facility of the University of Queensland (refer to Zhao et al. (2009)) for the details of this dating method). Details of the TIMS U-Th dating laboratory procedure are provided by Yu et al. (2012), who dated over 100 coral samples from boulders on the southern Great Barrier Reef to examine the decadal variations in storm activity in the region over the past century.

It is assumed that live coral was dislodged from the upper living reef surface at the time of past extreme wave events when a boulder was transported. Thus, the age of the coral samples may be taken to represent the approximate timing of the event (Yu et al., 2009), or at least the minimum time that has passed since the event occurred. Timing of prehistorical extreme wave events inferred from boulder ages yielded by U-Th dating of constituent corals should be interpreted with caution, however, as challenges exist with this method. For example, on Taveuni Island (Fiji), Etienne and Terry (2012) showed that if the oldest instead of the youngest part of a large boulder is sampled for dating, the resulting 'boulder age' might be 250 years older than the actual boulder transport timing. On the Makemo reef flat, bioerosion is not intense and boulders are not severely weathered. Fossil coral growth directions can be identified on most boulders, therefore such age error is hopefully avoided.

Following the approach of Yu et al. (2012), the age error due to sample thickness was added to the age uncertainty range, because the dated material may not be the youngest part of the collected coral sample. In sample preparation, cubes of about 3 cm^3 were sent to the isotope facility for U-Th dating analyses. Growth rates of corals near Makemo Atoll are ~10 mm/year on average: e.g., on Moorea in the Society Islands, the average growth rate of the massive coral *Porites* was 10.7 mm/year over the period CE1800-1905 (Bessat and Buigues, 2001); on Tahiti, the mean aggradation rate of the robust-branching *Acropora* coral, which commonly dominates the upper fore reef, was 9.3–11 mm/year through the postglacial period from 14,000 BP (Montaggioni and Camoin, 1997). Each 3-cm thick sample therefore represents three years of coral growth, so an additional error of ±3 years was added to each dating result.

5. Results

5.1. Boulder distribution

A total of 286 boulders were recorded along the 15-km long northern Makemo reef flat (Fig. 7). Some of the largest clasts reached the

'meso-boulder' category (i.e. b-axis >4.1 m), following the scale of Terry and Goff (2014). A total of 45 (16%) clasts were over 20 m^3 in volume. The density of samples measured by both mass/volume and Archimedean methods were similar: 1.67 ± 0.2 g/cm^3 and 1.70 ± 0.3 g/cm^3, respectively. Thus, a rounded density value of 1.7 g/cm^3 was used for the determination of clast mass. The largest meso-boulder (7.5 × 5.5 × 3.35 m) had an estimated mass of 164.4 t; the smallest (0.77 × 0.68 × 0.66 m) 0.41 t (metric tons or tonnes, t). The mean (±standard deviation) volume and mass of all 286 boulders was 11.8 ± 11.3 m^3 and 20.0 ± 19.2 t respectively; the median (±median absolute deviation) volume was 8.9 ± 5.0 m^3 and median mass was 15.2 ± 8.4 t.

The majority of the boulders in all zones except zone B are orientated parallel to slightly sub-parallel to the shore (Table 3). The minimum distance between a measured clast and the reef edge was 11 m. The maximum distance was 162 m for a small spherical boulder (1.17 × 1.16 × 1.14 m; mass = 0.82 t) that was deposited behind the beach in the vegetation zone. The distribution of boulders on the coast follows a clear landward-fining trend (Fig. 8).

Of the 286 boulders investigated, 30 were emerged reef boulders. Sixteen of these were deposited on the reef top; the other 14 were washed farther landward on the beach surface. The 2nd and 7th largest boulders (84.5 t and 74.9 t) were reef top boulders, derived from the emerged reef. The other reef top boulders were of various sizes, with masses ranging from 1.2 to 33.0 t. Most of the large reef top boulders were situated in zone A in the western section of the studied shore. In contrast, the beach boulders were all small boulders weighing <4 t. Most (12 of 14) beach boulders were found in zone B with masses ranging between 0.4 and 2.2 t. The farthest landward boulder was situated 162 m from the reef edge and was 67 m from the emerged reef.

5.2. Flow velocity estimation

The minimum flow velocity (MFV) required to initiate the transport of the 256 reef-edge boulders range from 5.4–15.7 m/s. Velocities of only 1.5–4.4 m/s were sufficient to initiate the movement of the 30 emerged reef boulders by sliding. However, some emerged reef boulders showed evidence of rolling or lifting, e.g. one boulder sitting on top of another. Therefore, higher velocities associated with these transport modes were the assumed MFVs.

The MFVs calculated from boulders represent the flow generated by breaking waves at the boulder source where transport is initiated. Reef-edge boulders were considered to come from the nearest reef edge location. As numerous boulders were measured in this study, the Makemo reef edge was divided into 100-m intervals on the map for illustration and analyses (Fig. 9). The highest MFV calculated from all boulders within each 100-m section therefore represents a conservative estimate of the maximum flow that has impacted this section of the coastline. A flow velocity exceeding the highest MFV is assumed to be capable of initiating transport of all boulders in this 100-m section. For emerged reef boulders, it was difficult to identify the original source location and original transport direction, i.e. either by run-up or backwash. Evidence of run-up or backwash could be clearly identified for only four boulder sources on the emerged reef (labelled on Fig. 9). Coloured lines to indicate MFV are drawn at boulder locations when a boulder source is unknown.

The boulders that require highest MFVs for transport are clustered in zones D and E, where 19 out of 20 measured clasts required >13 m/s to be transported (Fig. 9). The exception is in the north-facing zone C. Despite the presence of large boulders in zone A, the largest of all were

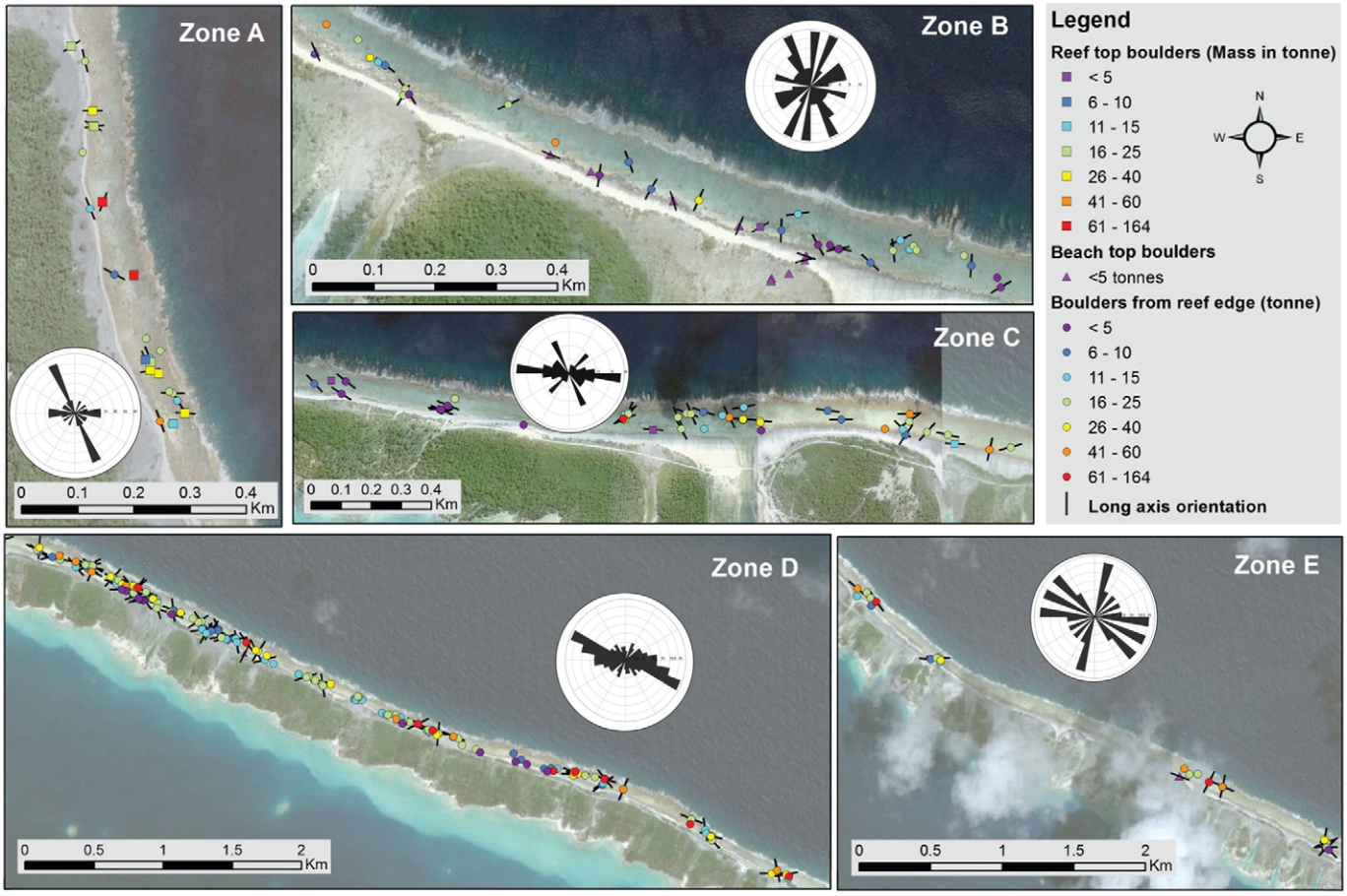

Fig. 7. Distribution, size, and orientation of boulders in Zones A to E on Makemo Atoll. See Fig. 2 for the location of each zone on the atoll. Rose diagrams of boulder orientation at each zone are displayed in circles. The boulder orientations were group into 10° grids for calculation. At all zones except B, the majority of the boulders are aligned with a-axes parallel to the shore. Refer to Lau et al. (2014) for more results and discussion on boulder orientation in the Makemo boulder field. (Satellite images from Google Earth).

Table 3
Shore and major boulder orientation of the divided zones A to E. The category for boulder orientation relative to the shore is divided in the same way as in Watt et al. (2010). Orientation within ±10° to shoreline orientation is considered 'shore parallel'; ±30° to shoreline is 'sub-parallel'.

Zone	A	B	C	D	E
Number of boulders	24	44	43	151	24
Mean boulder mass (t) ± standard deviation (t)	26.29 ± 18.65	10.08 ± 11.03	16.70 ± 15.04	21.43 ± 17.94	29.19 ± 33.44
Median boulder mass (t) ± median absolute deviation	21.02 ± 7.05	6.09 ± 4.66	12.24 ± 7.35	15.49 ± 8.00	17.98 ± 8.21
Shore orientation	160°	100°	90°	110°	115–135°
Major boulder orientation (relative to shore)	150°–160° (Parallel)	None	90°–100° (Parallel)	100°–120° (Parallel)	90°–140° (Parallel to sub-parallel)

derived from the emerged reef, thereby requiring lower MFVs for transport by sliding or rolling. Regarding wave direction, all boulders that required MFVs over 14 m/s were deposited on the northeast-facing coast. The north-facing coastline had been impacted by waves with MFV of 13.3 m/s, whilst on the east-facing coast there is no boulder that required an MFV > 12.1 m/s. From the limited number of backwash boulders identified, the backwash MFV was determined to be >4.8 m/s on the north-facing coast of Makemo.

5.3. Ages of carbonate boulders

The calendar ages of the 20 dated boulders range from CE132 ± 93 to CE1882 ± 6 (Table 4). Seven coral samples were altered, thereby suffering severe uranium loss. Therefore, their resulting ages were treated as maximums. Two of these altered samples, A039 and C075, were obtained from emerged reef boulders, as inferred from their shapes and resemblance to the local in situ emerged reefs. As the reefs emerged from seawater before boulder detachment, the dated coral mortality ages are not representative of the age of wave events, but probably the time of reef emergence.

Besides the altered coral samples, 13 pristine (unaltered) samples were all dated to the last millennium. Their ages are of high resolution with an estimated error range of less than ±9 years, including the additional ±3 year sample error (see Section 4.4). Eight samples were dated within the period CE1700–1900, with two youngest boulders dating to CE1883 ± 6 (Table 4).

6. Discussion

6.1. Emerged Holocene landforms as boulder sources

The coastal landscape of zone A differs notably from other zones on Makemo. Large boulders were so numerous on both the reef flat and the beach that only the largest were selected for measurement. The presence of this many larger boulders initially seems to support the assumption that extreme waves are be more frequent on this section of the coast than elsewhere. However, a segment of emerged reef remnant overlain by calcareous beachrock of approximately 0.5 m thickness crops out on the modern reef flat close to the beach. Such a feature necessitated reconsideration of the possible boulder source. This beachrock of coral conglomerate formed when the sea level was higher. When reef materials are wetted sufficiently in the intertidal zone, calcareous cement precipitates between the sediments and binds them together (Stoddart and Cann, 1965; Murphy, 2009). A satellite image of the area in question shows the arc-shaped band of emergent beachrock follows the curvature of the modern beach (Fig. 10a–b). The upper surface is inclined towards the sea, resembling a beach slope. The markedly lower number of boulders on the section of reef flat with emerged

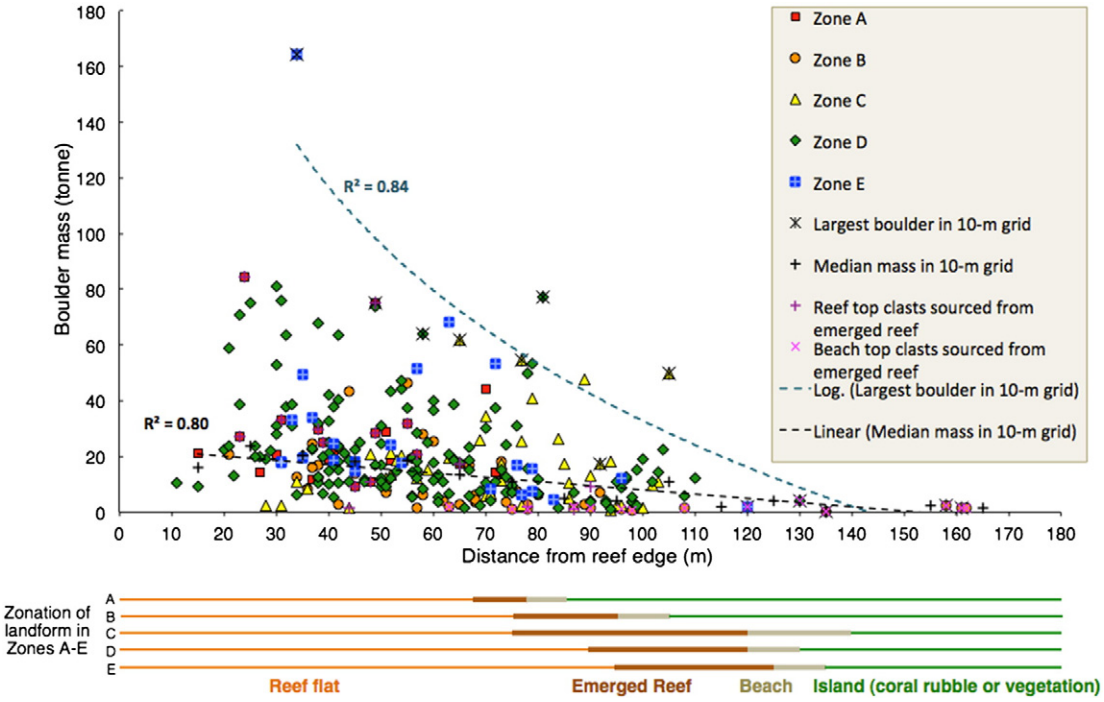

Fig. 8. Mass versus distance from the reef edge for the boulders measured on the Makemo shore. A clear landward fining trend is exhibited in the arrangement of 286 measured boulders. Strong logarithmic and linear relationships ($R^2 = 0.84$ and 0.80) are present among the largest boulders in 10-m increments and the median boulder mass in each 10 m grid. Boulders situated within 30 m from the reef edge were excluded in the largest boulder correlation plotting because clasts close to the reef edge are probably remobilized by waves more frequently.

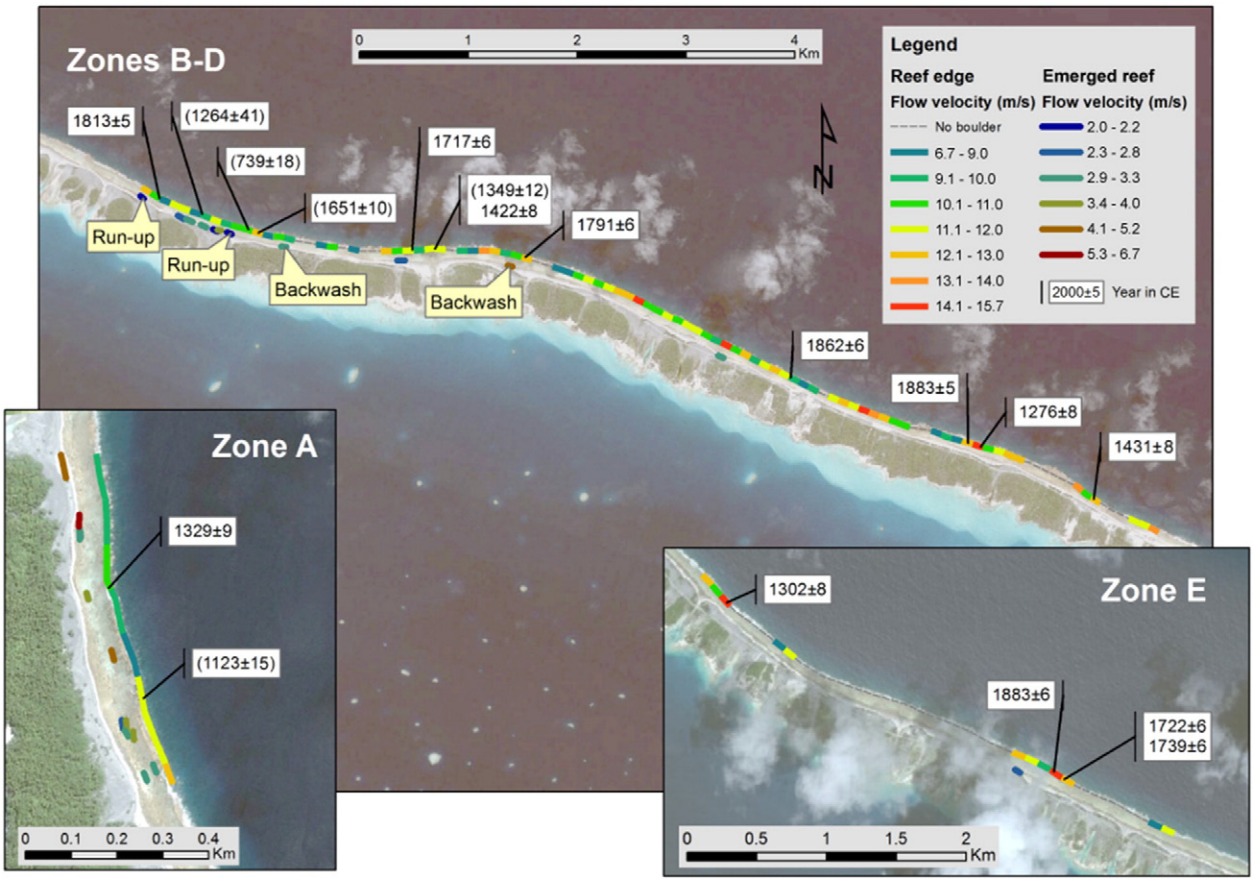

Fig. 9. Minimum flow velocities (MFVs) along the studied reef of Makemo Atoll. The boundary of the reef edge is divided into 100-m sections for displaying the variation of MFV required to transport boulders sourced from the living reef framework. MFVs required to move boulders sourced from the emerged reef are indicated by lines drawn at the boulder location on the reef flat. Dated coral mortality ages with error range (years in CE) are given in white boxes. Dates in brackets are from weathered (altered) coral samples thus their ages should be considered as maximum age only.

beachrock remaining intact suggests, conversely, that many boulders elsewhere in zone A once formed the emerged beachrock, which has subsequently broken apart (Fig. 10c).

In zones B–E, emerged reefs are also partly preserved. Here, the lack of beachrock implies that emerged reefs may have been broken into smaller pieces by wave impact, leaving no large emerged reef boulders

Table 4
Coral mortality age of 20 carbonate boulders on Makemo.

Zone/boulder ID	Distance from reef edge (m)	Dimension (m)	Volume (m^3)	Mass (tonnes)	U-Th corrected age (yr)	Calendar age (CE)
D169	23	4.78 × 4.56 × 2.73	41.7	70.8	736.8 ± 4.6	1276 ± 8
E146	34	7.50 × 5.50 × 3.35	96.7	164.5	711.2 ± 5.4	1302 ± 8
A040	72	4.11 × 2.55 × 1.14	8.3	14.2	683.4 ± 6.1	1329 ± 9
C058	79	5.20 × 4.10 × 1.61	24	40.8	591.4 ± 5.4	1422 ± 8
D155	23	4.17 × 3.62 × 2.15	22.8	38.7	582.5 ± 4.8	1431 ± 8
C051	48	4.56 × 3.03 × 1.25	12.1	20.6	296.0 ± 2.9	1717 ± 6
E129	35	5.51 × 3.68 × 2.05	29.1	49.5	291.6 ± 3.3	1722 ± 6
E130	41	4.31 × 2.84 × 1.70	14.6	24.8	274.7 ± 3.2	1739 ± 6
C076	89	5.98 × 4.91 × 1.37	28.1	47.8	221.9 ± 3.0	1791 ± 6
B108	73	4.48 × 3.25 × 1.06	10.8	18.3	200.4 ± 2.4	1813 ± 5
D183	41	5.34 × 4.71 × 1.27	22.3	38	150.8 ± 3.2	1862 ± 6
D172	81	6.93 × 5.95 × 2.20 [T]	45.4	77.2	130.8 ± 1.9	1883 ± 5
E131	63	7.10 × 3.89 × 2.05 [T]	40	68	130.3 ± 2.7	1883 ± 6
Uncertainty in age estimate:						
C075	90	5.66 × 2.35 × 1.14 [T]	7.6	12.9	1878.4 ± 90.0	132 ± 93[a,b]
B083	38	4.24 × 3.73 × 1.26 [T]	10	17	1272.4 ± 15.1	739 ± 18[b]
A043	41	4.49 × 4.11 × 1.35 [T]	12.5	21.3	889.5 ± 12.1	1123 ± 15[b]
B118	76	2.47 × 1.86 × 1.35	4.3	7.4	744.4 ± 38.1	1264 ± 41[b]
C059	84	4.60 × 3.10 × 1.55	15.5	26.3	663.7 ± 8.8	1349 ± 12[b]
B081	21	3.67 × 3.26 × 2.04 [T]	12.2	20.7	362.2 ± 6.7	1651 ± 10[b]
A039	49	8.94 × 5.87 × 1.20	44.1	75	319.4 ± 10.0	1693 ± 13[a,b]

[T] indicates a triangular boulder.
[a] The ages of the two boulders derived from emerged reef are not representative of the wave event age.
[b] The ages for seven altered samples due to weathering and suffering from U loss should be regarded as maximum age only.

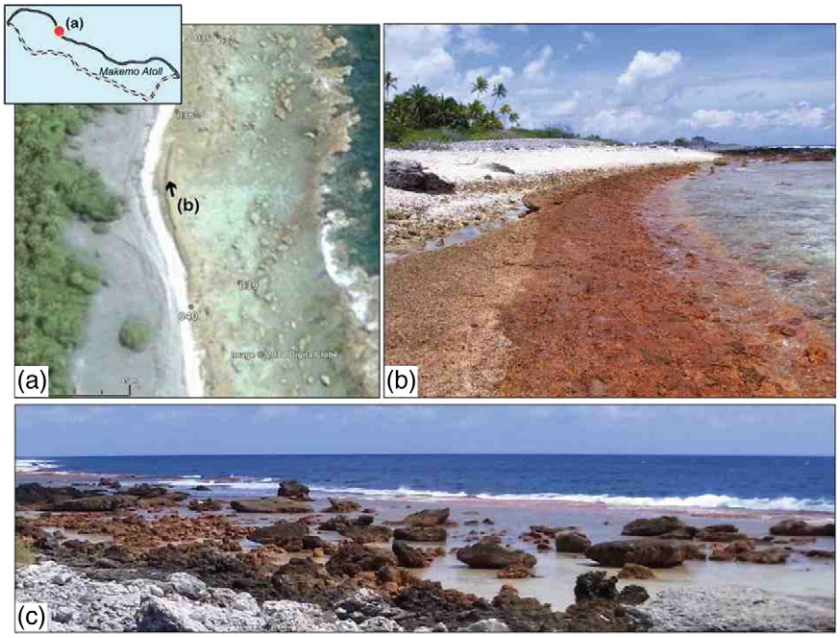

Fig. 10. (a) Satellite image showing the arc-shaped emerged beachrock segment in zone A (Image from Google Earth). The arrows indicate the directions of view in the following photos. (b) The calcareous beachrock band is inclined towards the sea with a top surface smoother than emerged reefs observed in other zones. (c) Abundant boulders present on the reef flat of zone A where emerged in situ beachrock and reef are not preserved. Many of these flat clasts were probably eroded from the emergent beachrock that once existed at the locality.

in these zones. The smaller boulders derived from the emerged reef are less well preserved, as they are easily eroded into smaller clasts or washed away by backwash. This example highlights the fact that the presence of large boulders, and/or many boulders at any one locality, does not necessary indicate unusually strong or high wave impact. One must consider the boulder source and lithology from field observations to interpret wave transport.

Determining the transport direction of reef top boulders derived from the emerged coastal landforms is especially challenging. These boulders are located seaward of the in situ emerged reef and therefore appear to have been transported by backwash. Alternatively, they were also possibly detached from the emerged reef earlier, when the emerged landforms extended further on the reef flat. Subsequently after boulder detachment, they could be transported by either run-up or backwash flow to their current locations.

6.2. Boulder distributions

As illustrated in Fig. 8, carbonate boulders studied on Makemo show an overall logarithmic landward-fining trend. Similar, but exponential, fining trends were identified in a storm wave boulder field on Kudaka Island of Japan (Goto et al., 2009). On the other hand, tsunami boulder fields may show fining or coarsening trends in the landward direction, or boulders may be scattered randomly on the coast (Goto et al., 2012). It has also been reported that tsunami waves with longer periods than storm waves can transport boulders as far as 1200 m inland from the reef edge, far beyond the landward limit of storm waves (Goto et al., 2010). However, narrow subaerial reefs on Makemo are not so favourable for preserving the signatures of tsunami-transported boulders. The width of the atoll rim studied only extends to a maximum of 600 m from reef edge to the lagoonal beach at some points of the atoll rim. Boulders transported over longer distance would be deposited in the lagoon and be difficult to identify as evidence of extreme waves. From both field observations and examination of satellite images, no boulders were visible beyond 170 m from reef edge, on the lagoonal beach or in the central lagoon. Thus, boulder distribution is not indicative of the cause of this boulder field (tsunami versus storm), as no subaerial preservation sites extend beyond the limit of boulder transport by storm waves.

Boulder reworking is another influence that limits the usefulness of boulder distributions for answering the storm-versus-tsunami question. The variety of dates from coral dating indicates that multiple extreme wave events have impacted this atoll. Thus, many of the older boulders deposited have potentially been remobilized during subsequent events. The lack of preferred boulder orientation in zone B is also likely due in part to boulder reworking. Boulders in this zone are smaller, meaning they can be remobilized or rotated by lower-energy waves more easily and frequently than in other zones. However, there is no evidence on Makemo showing boulder orientation is a reflection of boulder transport mode (Lau et al., 2014). Instead, the mostly parallel-to-shore boulder orientation suggest that large boulders were transported by extreme waves that approached normal to shore. Hence, the northeast waves on Makemo produced MFVs at least 15.7 m/s, while waves coming from north and east were of similar magnitude with MFVs over 13.3 m/s and 12.1 m/s respectively.

Since the subaerial windward island of Makemo is only present at the northern shore along NW-SE, the atoll is only exposed to extreme waves coming from north to east directions. This is one reason for the absence of boulders from the 1982–83 cyclone season. Large boulders were deposited on the western and north-western rims of other Tuamotu atolls by these recent cyclonic waves, indicating the strongest waves in the season were from the west. This highlights that if analysis of extreme waves affecting the Tuamotus from all directions is desired, then it is important to investigate more atolls of different orientations.

Flow velocity estimation reveals that 20 investigated boulders required MFVs over 14 m/s to be transported onto the reef flat. Such a calculated flow velocity is comparable to recent extreme wave events such as the 2004 Indian Ocean Tsunami, when the estimated maximum current velocity was 8–15 m/s on the reef edge at Pakarang Cape, Thailand (Goto et al., 2007). It is also near to the estimated flow velocity (before wave breaking) of 16.67 m/s generated by Tropical Cyclone Krosa, which impacted northeast Taiwan in 2007 and generated a record wave height of 32.3 m offshore in shallow ocean (Liu et al., 2008; Babanin et al., 2011).

6.3. Boulder ages

Two emerged reef boulders were dated for coral mortality age. While both altered samples do not give precise U-Th ages, the sample from boulder C075 yielded a maximum age of CE132 ± 93, which is possibly the age of the Holocene emerged reef when the sea level was more than 1.1 m above the present sea level. However, the maximum age of boulder A039 was CE1693 ± 13, which is too young to be the formation age of the reef at the locality, because the sea level at that time is estimated at less than 0.3 m above modern sea level (Dickinson, 2003). One explanation for this discrepancy might be that this altered sample has been contaminated by younger carbonate materials on the reef. As the ages of altered coral samples have a large degree of uncertainty and only indicate maximum age, their ages are not considered further.

From the measured dates of 13 "pristine" coral samples, three groups of boulders were determined to be of a similar age. These findings reveal possibly five to nine extreme wave events producing MFVs >8 m/s between CE1200 and 1900 (Fig. 11). Also, similar MFV ranges are required to move boulders of comparable ages. For example, one boulder pair from the event dating to approximately CE1425 required MFVs of 10.9–12.6 m/s. Boulders emplaced around CE1720 required flows of 9.6–12.3 m/s. Finally, the boulder pair dated from CE1883 indicates higher MFVs of 12.7–14.6 m/s.

6.4. Occurrence of extreme wave events

6.4.1. Comparison with historical storm records

The youngest boulder age on Makemo is CE1883. The earliest recorded storm in the Tuamotus can be traced to CE1822. Thus, there are roughly 60 years of overlapping historical and geological records. According to written sources, cyclones struck the Tuamotus in CE1822, CE1825, and three times during CE1877–78 (Sachet, 1983). Two boulder ages of CE1883 ± 6 match three recorded cyclones over CE1878–88, among which the cyclone on 6–7 February 1878 was believed to be the most intense (Sachet, 1983). Furthermore, as no historical event corresponds to the CE1862 ± 6 sample, this boulder probably represents the same CE1878 event. The severe cyclone in 1878 was reportedly extremely violent with powerful waves that swept across the Tuamotus, especially in the west (Gordon-Cumming, 1882, cited in d'Aubert and Nunn, 2012; Stoddart, 1969; Sachet, 1983). It was described that "*Nothing of the sort has occurred in these seas in the present century*" (Gordon-Cumming, 1882:353–360, cited in d'Aubert and Nunn, 2012).

On Kaukura Atoll "*A strong easterly breeze had for three consecutive days lashed the waters of the lagoon into fury, then gradually veered round to the west with ever increasing force. The ground was apparently about to be wholly submerged*" and some people "*fled to the highest part of the land, which was about fifteen feet* [4.57 m] *above the ordinary water level. The ground was strewn with large rocks and stumps of palm trees. To these they clung all through the night, while the waves from both lake* [*lagoon*] *and sea met and dashed right over them in cataracts of foam*", the water only receded from the island "*when morning broke*" (Gordon-Cumming, 1882:353–360, cited in d'Aubert and Nunn, 2012).

The extremely powerful waves produced by this cyclone were felt not only on Kaukura, located about 350 km west of Makemo, but also on Raroia, 130 km northeast of Makemo, where two boats were pushed inland (Giovanelli, 1940, cited in d'Aubert and Nunn, 2012). As waves and water level were exceptionally strong and high on atolls near Makemo, the impact of waves persisted, and the islands flooded to a depth of a few metres through the night. It is possible that two boulders, weighing 77 and 68 t, on the northeast-facing reef flat were emplaced by waves of this event in 1878. In this case, the MFVs during this cyclone may have reached at least 14.6 m/s at the reef edge—as estimated from the large boulders measured in this study (Fig. 11).

Although written records of storms do not extend back to the 18th century, geomorphic evidence and boulders on other Tuamotu atolls suggest the occurrence of at least one cyclone event in this prehistoric period. By examining coastal geomorphology on satellite images of multiple atolls in the Tuamotus and carbon-14 dates of boulders, Hyvernaud (2009) proposed the occurrence of a cyclone in CE1715 ± 60 (cited in Etienne et al., 2011). Despite the large error range in the carbon-14 dating results, this cyclone event age is consistent with our U-Th dates of two boulders (CE1717 ± 6 and CE1722 ± 6). Moreover, an additional U-Th date of CE1739 ± 6 also falls within this time period. Given the uncertainty, additional boulder age data should be collected from other Tuamotu atolls to better validate this pre-historical cyclone event.

6.4.2. Comparison with tsunami records

The earliest written record of a tsunami in the Tuamotus dates from CE1946, which post-dates the youngest coral mortality age of our

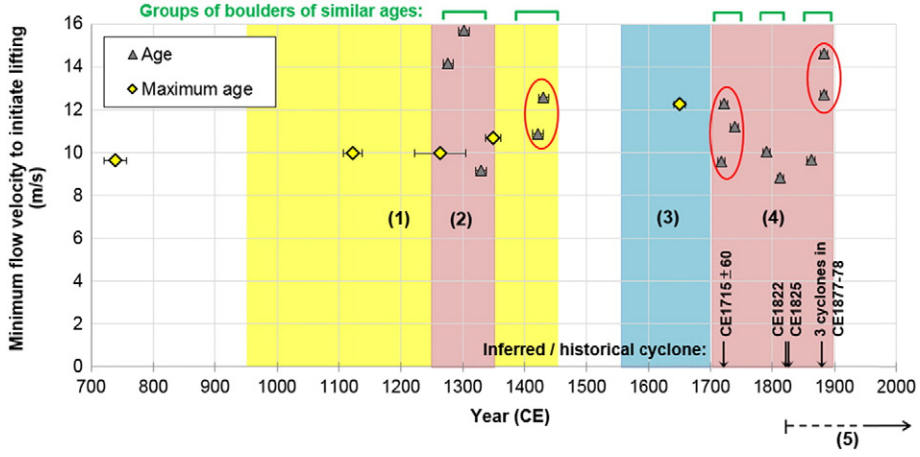

Fig. 11. Coral mortality ages of 18 boulders derived from the living reef framework and the respective MFV required to lift them onto the reef flat. Boulder groups of same age range are circled in red, boulders in each group are highly likely produced by the same event. Groups of roughly similar ages are indicated by green brackets above graph, these boulders were possibly derived from the same event. Overall, 13 high resolution boulder dates suggest 5–9 occurrences of extreme wave events from CE1200–1900. Five periods with climatic conditions that may affect storm activity according to existing literature are labelled on the graph: (1) (shaded yellow) High cyclone activity in the central South Pacific 1000–500 BP (Toomey et al., 2013); (2) (pink) High storminess in the Pacific around CE1250–1350 (Nunn, 2007); (3) (blue) Cooler sea-surface temperatures from CE1565–1700, (4) (pink) Higher temperatures in the 18th–19th centuries at the Great Barrier Reef (Hendy et al., 2002); (5) (below x-axis) Historical time with probably incomplete written records of wave events starting CE1822. The inferred cyclone in the Tuamotus proposed by Hyvernaud (2009), and five historical cyclones in period (5) are also labelled.

boulder samples. Taking oral records into account, a tsunami that apparently occurred in the 16th century that destroyed Rangiroa Atoll is not represented in our dataset. Similarly, while there were multiple inferred tsunami occurrences in other parts of French Polynesia in the 15th and 16th centuries, which were possibly triggered by earthquakes at the Tonga-Kermadec Trench (TKT) or South America (refer to Table 2), no sampled boulder on Makemo dates to these two centuries.

Two CE1883 boulders coincide with the global tsunami generated from the Krakatau volcanic eruption in Indonesia. However, we reject the idea that these large boulders might have resulted from the Krakatau tsunami. Waves from Krakatau propagated from Java to the east into the Indian Ocean, but the Pacific Ocean was not greatly affected. Tide gauge records showed only minor water fluctuations along Pacific shorelines. For instance, waves of 0.1 m, 0.24 m and 0.3 m were detected at Sydney (Australia), Oahu Island (Hawaii), and New Zealand (city not specified), respectively (Iida et al., 1967).

6.4.3. Comparison with late-Holocene climate variability

In this study, only a small number of boulder dates can be compared with written or oral records, and most events mentioned in historical records are not represented by our measured boulder ages. Nonetheless, on longer timescales, there appears to be a reasonable association between Makemo boulder ages and records of climatic variability over the last millennium.

In attempting to reconstruct tropical cyclone activity in the central South Pacific for the mid-late Holocene, Toomey et al. (2013) analysed coarse-grained washover sediments in the deep back-reef lagoon on Tahaa, a volcanic island northwest of Tahiti. They then compared the stratigraphic record with boulder dates obtained from other parts of French Polynesia as reported by Pirazzoli et al. (1987a, 1988a). In contrast with the high-resolution U-Th dates of our Makemo boulders, all boulder dates presented in older literature were obtained from carbon-14 dating with age errors of over 50 years. Four reef boulders dated from the Tuamotus are older than 1000 years BP (Pirazzoli et al., 1988a; Toomey et al., 2013). Although stratigraphic records suggested that cyclone activity was high in the region over 1000–500 BP (Fig. 11), no previously boulder dated from this period to support this finding. The work presented herein is therefore valuable because our younger boulder dates on Makemo fill this gap by providing five high-resolution dates within this 500-year timespan.

Moreover, the largest boulder on Makemo dates to CE1302 ± 5, coinciding with an apparent period of increased storminess in the area of many low Pacific islands around CE1300 (Nunn, 2007). It has been proposed that between the Medieval Warm Period (MWP) and the Little Ice Age (LIA), there was a transition period (around CE1250–1350 in the Pacific Basin) of abrupt climate change resulting in increased storminess and precipitation in several parts of the world (Grove, 1988; Stine, 1990; Goodwin et al., 2004; Nunn, 2007). On a number of Pacific islands, including Tahiti, Huahine and Moorea in French Polynesia, soil loss from interior highlands, and the concurrent accumulation of sediment on lowlands, were inferred as evidence of high precipitation and storms during the 14th century (Orliac, 1997; Nunn, 2007). Nunn (2007), making reference to Henry (1951), suggested that the strongest storm on Tahiti in this period may have been recorded in local traditional folklore as a 'deluge myth'. Accepting the occurrence of this climatic transition phase CE1250–1350, we can infer that three boulders with dates CE1276 ± 8 (71 t), CE1302 ± 8 (164 t) and CE1329 ± 9 (14 t) were emplaced onto the Makemo reef flat by exceptional waves during this stormy climatic interlude.

Of further interest, no boulder dates fall within the approximately 280-year period extending from CE1436 to 1718, a period coinciding with the LIA, when temperatures in many parts of the world were as much as 1 °C cooler than the 20th century mean (Nunn, 2007) (Fig. 11). The absence of coastal boulders during this time may indicate a reduced storminess in the Tuamotus owing to cooler sea-surface temperatures (SSTs) around the Western Pacific Rim (Hendy et al., 2002; Evans et al., 2002), a condition that favoured neither storm formation nor storm tracking farther eastwards into the Central Pacific. Coral isotope records have shown that SSTs at the Great Barrier Reef were ~0.2–0.3 °C cooler during CE1565–1700 than the 420-year average (Hendy et al., 2002). In contrast, between CE1700 and the 1870s, SSTs at the Great Barrier Reef and Rarotonga Island in the Cook Islands were above average, before cooling in the early 1900s (Hendy et al., 2002). Again our Makemo boulder evidence matches well with these stages of relative cooling and warming in the western and central South Pacific: no boulders (except one altered sample) date from the cool periods, but eight boulders representing three to five individual extreme wave events, occurred in the warm period over the 18th and 19th centuries. This positive association between Great Barrier Reef SSTs and occurrences of extreme wave events at Makemo suggest that the majority of boulders were emplaced onto the reef flat by cyclonic waves during phases of high storminess in the central South Pacific Ocean.

7. Conclusions

Atolls in the Tuamotu Archipelago of French Polynesia in the central South Pacific are situated far from major tsunamigenic subduction zones and are infrequently affected by tropical cyclones, as compared with island groups farther west in the South Pacific. Thus, few very intense cyclones have been recorded in the central South Pacific over the past century, while boulder and other sedimentary data in existing literature have shown how gaps of over 100 years are not unusual between extreme wave events. Yet, our investigation of the numerous large carbonate boulders on Makemo Atoll reveals that extreme wave events prior to the modern record were of a greater magnitude than during the past century. Many boulder ages obtained are too old to compare with historical cyclone and tsunami records, but they nonetheless coincide with apparent periods of increased storminess in the late Holocene, when strong cyclones were more frequent. Boulder ages suggest possibly 5–9 extreme wave events with minimum flow velocities over 8 m/s have struck the atoll between CE1200 and 1900, with 3–5 events occurring over the two centuries CE1700–1900. The two youngest boulders with minimum flow velocities >14 m/s were likely produced by the intense cyclone of February 1878, which flooded many atolls in the western Tuamotus. The Makemo boulders examined herein aid in reconstructing the variability in cyclone activity over the last millennium. This work therefore underscores the value of coastal boulder studies as part of multi-proxy investigations that aim to illuminate palaeo-cyclone activity over centennial timescales.

Existing literature, historical records and observations over the past century all indicate that El Niño conditions are most favourable for cyclone occurrence in the central South Pacific region. Over longer timescales, higher sea-surface temperatures also favour greater cyclone activity near the Tuamotu Archipelago. If SSTs rise through the 21st century as projected by the IPCC (2014), another period of increase storminess in the central South Pacific may ensue. Even for distant cyclones, strong swells have the potential to inundate low-lying atolls. For Makemo Atoll, cyclone-generated extreme wave events can potentially recur again in future—perhaps comparable to the powerful cyclone of February 1878 that generated flow velocities over 14.6 m/s on Makemo's northern coast. This threat also pertains to the northern shores of other atolls in the Tuamotus. Coastal vulnerability assessments would therefore benefit from taking this information into account.

Acknowledgements

We thank the two anonymous reviewers whose comments helped improve this manuscript. Fieldwork by S Etienne and AYA Lau was supported by CPER-Rinalpof grant (French Government and Territory of French Polynesia). AYA Lau was supported by the National University of Singapore Research Scholarship. JP Terry was supported by the Singapore Ministry of Education Tier 1 research grant no. FY2012-

FRC2-005 and Zayed University RIF grant no. R15053. The contribution of A Switzer and Y Lee was supported by the Singapore National Research Foundation under its NRF Fellowship scheme (National Research Fellow Award No. NRF-RF2010-04) and administered by the Earth Observatory of Singapore. This is Earth Observatory of Singapore contribution 57.

References

Allan, R.J., Nicholls, N., 1991. A further extension of the Tahiti-Darwin SOI, early ENSO events and Darwin pressure. J. Clim. 4, 743–749.

Andréfouët, S., Ardhuin, F., Queffeulou, P., Le Gendre, R., 2012. Island shadow effects and the wave climate of the Western Tuamotu Archipelago (French Polynesia) inferred from altimetry and numerical model data. Mar. Pollut. Bull. 65, 415–424.

Araoka, D., Yokoyama, Y., Suzuki, A., Goto, K., Miyagi, K., Miyazawa, K., Matsuzaki, H., Kawahata, H., 2013. Tsunami recurrence revealed by Porites coral boulders in the southern Ryukyu Islands, Japan. Geology 41, 919–922.

Babanin, A.V., Hsu, T.W., Roland, A., Ou, S.H., Doong, D.J., Kao, C.C., 2011. Spectral wave modelling of typhoon Krosa. Nat. Hazards Earth Syst. Sci. 11, 501–511.

Bessat, F., Buigues, D., 2001. Two centuries of variation in coral growth in a massive Porites colony from Moorea (French Polynesia): a response of ocean–atmosphere variability from south central Pacific. Palaeogeogr. Palaeoclimatol. Palaeoecol. 175, 381–392.

Bourrouilh-Le Jan, F.G., Talandier, J., 1985. Sédimentation et fracturation de haute énergie en milieu récifal: tsunamis, ouragans et cyclones et leurs effets sur la sédimentologie et la géomorphologie d'un atoll: motu et hoa, à Rangiroa, Tuamotu, Pacifique SE. Mar. Geol. 67, 263–333.

Bruckner, A.W., 2014. Global Reef Expedition: Tuamotu Archipelago, French Polynesia. Field Report. Khaled bin Sultan Living Oceans Foundation, Landover MD 23 pp.

Camoin, G.F., Ebren, P., Eisenhauer, A., Bard, E., Faure, G., 2001. A 300 000-yr coral reef record of sea level changes, Mururoa atoll (Tuamotu Archipelago, French Polynesia). Palaeogeogr. Palaeoclimatol. Palaeoecol. 175, 325–341.

Canavesio, R., 2014. Estimer les houles cycloniques à partir d'observations météorologiques limitées: exemple de la submersion d'Anaa en 1906 aux Tuamotu (Polynésie française). VertigO 14, 3 December 2014, online 12 Jan 2015. (Available at:) http://vertigo.revues.org/15375.

CEA, 2009. Earthquake of Magnitude Mw = 8.2 in the Samoa Islands (Pacific). (Available at:) http://www-dase.cea.fr/actu/dossiers_scientifiques/2009-09-30/index_en.html.

CEA, 2010. Magnitude Mw = 8.8 Earthquake in Chile (115 km NNE of Concepción) on 27 February 2010 and Pacific-wide Tsunami. (Available at:) http://www-dase.cea.fr/actu/dossiers_scientifiques/2010-03-01/index.html.

Chappel, L.C., Bate, P.W., 2000. The South Pacific and southeast Indian Ocean tropical cyclone season 1997-98. Aust. Met. Mag. 49, 121–138.

Clague, D.A., Jarrard, R.D., 1973. Tertiary Pacific plate motion deduced from the Hawaiian-emperor chain. Bull. Geol. Soc. Am. 84, 1135–1154.

Climatic Prediction Center, N.O.A.A., 2015. Historical el Nino/La Nina episodes (1950-present). http://www.cpc.noaa.gov/products/analysis_monitoring/ensostuff/ensoyears.shtml (Accessed: 15 June 1015).

Damlamian, H., Kruger, J., Turagabeci, M., Kumar, S., 2013. Cyclone Wave Inundation Models for Apataki. Arutua, Kauehi, Manihi and Rangiroa Atolls, French Polynesia.

D'Aubert, A.M., Nunn, P.D., 2012. Furious Winds and Parched Islands: Tropical Cyclones (1558–1970) and Droughts (1722–1987) in the Pacific (Xlibris).

DeAngelis, D., 1983. Hurricane alley. Mariners Weather Log 27 (106–109), 172–176.

des Garets, E., 2005. Bilan des connaissances sur les surcotes marines en Polynésie. Rapport BRGM/RP-55038-FR.

D'Hauteserre, A., 1978. Le climat de la Polynésie Francaise. Monographie 107 de la Météorologie National. pp. 1–67.

Dickinson, W.R., 2001. Paleoshoreline record of relative Holocene sea levels on Pacific islands. Earth-Sci. Rev. 55, 191–234.

Dickinson, W.R., 2003. Impact of mid-Holocene hydro-isostatic highstand in regional sea level on habitability of islands in Pacific Oceania. J. Coast. Res. 19, 489–502.

Dupon, J.F., 1986. Atolls and the cyclone hazard: a case study of the Tuamotu Island. Environmental Case Study 3. New Caleonia, SPREP, South Pacific Commission, Noumea.

Editor of The Nautical Magazine, 1986. The Nautical Magazine and Naval Chronicle for 1856, London.

Engel, M., May, S.M., 2012. Bonaire's boulder fields revisited: evidence for Holocene tsunami impact on the Leeward Antilles. Quat. Sci. Rev. 1–16.

Etienne, S., 2012. Marine inundation hazards in French Polynesia: geomorphic impacts of Tropical Cyclone Oli in February 2010. In: Terry, J.P., Goff, J. (Eds.), Natural Hazards in the Asia-Pacific Region: Recent Advances and Emerging Concepts. Geological Society, London, Special Publications 361, pp. 21–39.

Etienne, S., Terry, J.P., 2012. Coral boulders, gravel tongues and sand sheets: features of coastal accretion and sediment nourishment by Cyclone Tomas (March 2010) on Taveuni Island, Fiji. Geomorphology 175-176, 54–65.

Etienne, S., Buckley, M., Paris, R., Nandasena, A.K., Clark, K., Strotz, L., Chagué-Goff, C., Goff, J., Richmond, B., 2011. The use of boulders for characterising past tsunamis: lessons from the 2004 Indian Ocean and 2009 South Pacific tsunamis. Earth Sci. Rev. 107, 76–90.

Etienne, S., Couchoud, I., Jeanson, M., Lau, A., Paris, R., Terry, J., 2014. Les risques naturels extrêmes sur les littoraux de la Polynésie française: Archives géologiques – modélisation – réduction des risques. Rapport scientifique du programme RINALPOF, Contrat de Projet Etat-Territoire 2009–2013. Université de la Polyiésie française – Ecole Pratique des Hautes Etudes, p. 98.

Evans, M.N., Kaplan, A., Cane, M.A., 2002. Pacific sea surface temperature field reconstruction from coral δ18O data using reduced space objective analysis. Paleoceanography 17, 1007.

Frohlich, C., Hornbach, M.J., Taylor, F.W., Shen, C.-C., Moala, A., Morton, A.E., Kruger, J., 2009. Huge erratic boulders in Tonga deposited by a prehistoric tsunami. Geology 37, 131–134.

Gienko, G.A., Terry, J.P., 2014. Three-dimensional modeling of coastal boulders using multi-view image measurements. Earth Surf. Process. Landf. 39, 853–864.

Gill, J.P., 1994. The South Pacific and southeast Indian ocean tropical cyclone season 1991–92. Aust. Meteorol. Mag. 43, 181–192.

Giovanelli, J.L., 1940. Les cyclones en Océanie française. Bulletin de la Société des Études océaniennes 6 (7), 250–267.

Goff, J., Chagué-Goff, C., Dominey-Howes, D., McAdoo, B., Cronin, S., Bonté-Grapetin, M., Nichol, S., Horrocks, M., Cisternas, M., Lamarche, G., Pelletier, B., Jaffe, B., Dudley, W., 2011. Palaeotsunamis in the Pacific Islands. Earth Sci. Rev. 107, 141–146.

Goff, J., McFadgen, B.G., Chague-Goff, C., Nichol, S.L., 2012. Palaeotsunamis and their influence on Polynesian settlement. The Holocene 22, 1067–1069.

Goodwin, I.D., van Ommen, T.D., Curran, M.A.J., Mayewski, P.A., 2004. Mid latitude winter climate variability in the south Indian and southwest Pacific regions since 1300 AD. Clim. Dyn. 22, 783–794.

Gordon-Cumming, C., 1882. A Lady's Cruise on a French Man-of-War. Blackwood & Sons, London.

Goto, K., Chavanich, S.A., Imamura, F., Kunthasap, P., Matsui, T., Minoura, K., Sugawara, D., Yanagisawa, H., 2007. Distribution, origin and transport process of boulders deposited by the 2004 Indian Ocean tsunami at Pakarang Cape, Thailand. Sediment. Geol. 202, 821–837.

Goto, K., Okada, K., Imamura, F., 2009. Characteristics and hydrodynamics of boulders transported by storm waves at Kudaka Island, Japan. Mar. Geol. 262, 14–24.

Goto, K., Miyagi, K., Kawamata, H., Imamura, F., 2010. Discrimination of boulders deposited by tsunamis and storm waves at Ishigaki Island, Japan. Mar. Geol. 269, 34–45.

Goto, K., Sugawara, D., Ikema, S., Miyagi, T., 2012. Sedimentary processes associated with sand and boulder deposits formed by the 2011 Tohoku-oki tsunami at Sabusawa Island, Japan. Sediment. Geol. 282, 188–198.

Grove, J.M., 1988. The Little Ice Age. Methuen, London.

Harmelin-Vivien, M., Stoddart, D.R., 1985. Hurricane effects on coral reefs. Proceedings of the Fifth International Coral Reef Congress, Tahiti. 3, pp. 315–350.

Hendy, E., Gagan, M., Alibert, C., McCulloch, M., Lough, J., Isdale, P., 2002. Abrupt decrease in tropical Pacific Sea surface salinity at end of little ice age. Science 295, 1511–1514.

Henry, T., 1951. Tahiti Aux Temps Anciens. Société des Océanistes, Paris.

Hyvernaud, O., 2009. Dislocations des barrières récifales occasionnées par un cyclone de forte énergie. 11th Pacific Science Inter-Congress, Tahiti..

Iida, K., Cox, D.C., Pararas-Carayannis, G., 1967. Preliminary Catalog of Tsunamis Occurring in the Pacific Ocean. HIG-67-10. Hawaii Institute of Geophysics, University of Hawaii, Honolulu.

Intes, A., Caillart, B., 1994. Environment and biota of the Tikehau (Tuamotu Archipelago, French Polynesia). Atoll Res. Bull. 415, 1–38.

IPCC, 2014. Summary for policymakers. In: Climate Change 2014: Impacts, Adaptation, and Vulnerability. Part A: Global and Sectoral Aspects. Contribution of Working Group II to the Fifth Assessment Report of the Intergovernmental Panel on Climate Change [Field, C.B., V.R. Barros, D.J. Dokken, K.J. Mach, M.D. Mastrandrea, T.E. Bilir, M. Chatterjee, K.L. Ebi, Y.O. Estrada, R.C. Genova, B. Girma, E.S. Kissel, A.N. Levy, S. MacCracken, P.R. Mastrandrea, and L.L. White (eds.)]. Cambridge University Press, Cambridge, United Kingdom and New York, NY, USA, pp. 1–32.

Joint Typhoon Warning Center Tropical Cyclone Best Track Data Site. http://www.usno.navy.mil/NOOC/nmfc-ph/RSS/jtwc/best_tracks/ Accessed: 13 February 2014.

Jordahl, K., Caress, D., McNutt, M., Bonneville, A., 2004. In: Hekinian, R., Stoffers, P., Cheminee, J.L. (Eds.), Sea-Floor Topography and Morphology of the Superswell Region. Oceanic Hotspots, Intraplate Submarine Magmatism and Tectonism, pp. 9–28.

Kellum Ottino, M., 1971. Archéologie d'une Vallée des les Marquises. Publications de la Societe des Oceanistes 26. Musée de l'Homme, Paris.

Kench, P.S., McLean, R.F., Brander, R.W., Nichol, S.L., Smithers, S.G., Ford, M.R., Parnell, K.E., Aslam, M., 2006. Geological effects of tsunami on mid-ocean atoll islands: the Maldives before and after the Sumatran tsunami. Geology 34, 177–180.

Kench, P.S., Nichol, S.L., Smithers, S.G., McLean, R.F., Brander, R.W., 2008. Tsunami as agents of geomorphic change in mid-ocean reef islands. Geomorphology 95, 361–383.

Larrue, S., Chiron, T., 2010. Les îles de Polynésie française face à l'aléa cyclonique. VertigO 10, 3 December 2010, online 20 dec 2010. (Available at:) http://vertigo.revues.org/10558.

Lau, A.Y.A., Etienne, S., Terry, J.P., Switzer, A.D., Lee, Y.S., 2014. A preliminary study of the distribution, sizes and orientations of large reef-top coral boulders deposited by extreme waves at Makemo Atoll, French Polynesia. In: Green, A.N., Cooper, J.A.G. (Eds.), Proceedings 13th International Coastal Symposium (Durban, South Africa). Journal of Coastal Research, Special Issue Vol. 70, pp. 272–277.

L'Institut de la statistique de la Polynésie française, 2012. Population par Géographie administrative et par Age décennal. (Available at:) http://www.ispf.pf/bases/Recensements/2012/Donnees_detaillees/Population.aspx

Liu, P.C., Chen, H.S., Doong, D.J., Kao, C.C., Hsu, Y.J.G., 2008. Monstrous ocean waves during typhoon Krosa. Annales Geophysicae (European Geosciences Union) 26, 1327–1329.

Liu, E., Zhao, J., Clark, T.R., Feng, Y., Leonard, N.D., Markham, H.L., Pandolfi, J.M., 2014. High-precision U–Th dating of storm-transported coral blocks on Frankland Islands, northern Great Barrier Reef, Australia. Palaeogeogr. Palaeoclimatol. Palaeoecol. 414, 68–78.

Météo-France, 1995. Surcotes liées au passage d'un cyclone en Polynésie (rapport final).

Ministère Du Développement Durable, 2006. Plan de prévention des risques. Note méthodologique de réalisation Ddes Ccartes. BRGM, Papeete.

Moerenhout, J.A., 1937. Voyages aux îles du Grand Océan. 2 vols Paris.
Montaggioni, L.F., Camoin, G.F., 1997. Geology of Makatea Island, Tuamotu Archipelago, French Polynesia. In: Vacher, H.L., Quinn, T. (Eds.), Geology and Hydrogeology of Carbonate IslandsDevelopments in Sedimentology 54. Elsevier B.V., Amsterdam, The Netherlands, pp. 453–473.
Montaggioni, L.F., Richard, G., Bourrouilh-Le Jan, F., Gabrié, C., Humbert, L., Monteforte, M., Naim, O., Payri, C., Salvat, B., 1985. Geology and marine biology of Makatea, an uplifted atoll, Tuamotu Archipelago, central Pacific Ocean. J. Coast. Res. 1, 165–171.
Murphy, F.J., 2009. Motu. In: Billespie, R.G., Clague, D.A. (Eds.), Encyclopedia of Islands. University of California Press, Berkeley, pp. 641–643.
Nakamura, M., Arashiro, Y., Shiga, S., 2014. Numerical simulations to account for boulder movements on Lanyu Island, Taiwan: tsunami or storm? Earth, Planets and Space 66, 128.
Nandasena, N.A.K., Paris, R., Tanaka, N., 2011. Reassessment of hydrodynamic equations: minimum flow velocity to initiate boulder transport by high energy events (storms, tsunamis). Mar. Geol. 281, 70–84.
NOAA National Climatic Data Center, 2014. International Best Track Archive for Climate Stewardship (IBTrACS). http://www.ncdc.noaa.gov/ibtracs/index.php (Accessed: 19 February 2014).
Nott, J., 1997. Extremely high-energy wave deposits inside the Great Barrier Reef, Australia: determining the cause—tsunami or tropical cyclone. Mar. Geol. 141, 193–207.
Nunn, P.D., 2007. Climate, Environment and Society in the Pacific during the Last Millennium. Elsevier, Amsterdam, The Netherlands.
Orliac, M., 1997. Human occupation and environmental modifications in the Papeno'o Valley, Tahiti. In: Kirch, P.V., Hunt, T.L. (Eds.), Historical Ecology in the Pacific Islands. Yale University Press, Connecticut, pp. 200–229.
Ottino, P., 1965. Ethno histoire de Rangiroa. Centre O.R.S.T.O.M, Papeete.
Pacific Tsunami Warning Center, 2011. (Available at:) http://ptwc.weather.gov/text.php?id=pacific.2011.03.12.063606.
Paris, R., Fournier, J., Poizot, E., Etienne, S., Morin, J., Lavigne, F., Wassmer, P., 2010. Boulder and fine sediment transport and deposition by the 2004 tsunami in Lhok Nga (western Banda Aceh, Sumatra, Indonesia): a coupled offshore–onshore model. Mar. Geol. 268, 43–54.
Pirazzoli, P.A., Montaggioni, L.F., 1986. Late Holocene sea-level changes in the northwest Tuamotu islands, French Polynesia. Quatern. Res. 25, 350–368.
Pirazzoli, P.A, Montaggioni, L.F., 1988. Holocene sea-level changes in French Polynesia. Palaeogeogr. Palaeoclimatol. Palaeoecol. 68, 153–175.
Pirazzoli, P.A., Delibrias, G., Montaggioni, L.F., Saliège, J.F., Vergnaud-Grazzini, C., 1987a. Vitesse de croissance latérale des platiers et évolution morphologique récente de l'atoll de Reao, îles Tuamotu, Polynésie française. Annales de l'Institut océanographique 63, 57–68.
Pirazzoli, P.A., Montaggioni, L.F., Vergnaud-Grazzini, C., Saliege, J.F., 1987b. Late Holocene sea levels and coral reef development in Vahitahi Atoll, eastern Tuamotu. Mar. Geol. 76, 105–116.
Pirazzoli, P.A., Montaggioni, L.F., Salvat, B., Faure, G., 1988a. Late Holocene sea level indicators from twelve atolls in the central and eastern Tuamotus (Pacific Ocean). Coral Reefs 7, 57–68.
Pirazzoli, P.A., Koba, M., Montaggioni, L.F., Person, A., 1988b. Anaa Tuamotu Islands, central Pacific: an ancient rising atoll? Mar. Geol. 82, 261–269.
Revell, C.G., Goulter, S.W., 1986. South Pacific tropical cyclones and the southern oscillation. Mon. Weather Rev. 114, 1138–1145.
Reymond, D., Hyvernaud, O., Okal, E.A., 2012. The 2010 and 2011 tsunamis in French Polynesia: operational aspects and field surveys. Pure Appl. Geophys. 170, 1169–1187.
Ricard, M., 1985. Rangiroa atoll, Tuamotu archipelago. In: Delesalle, B., Galzin, R., Salvat, B. (Eds.), Fifth International Reef Congress, Tahiti. Vol 1, pp. 159–210.
Ruminski, M., 1990. Two unusual tropical cyclones in the southeast Pacific. Mon. Weather Rev. 119, 218–222.
Sachet, M., 1983. Takapoto Atoll, Tuamotu Archipelago: terrestrial vegetation and flora. Atoll Res. Bull. 277, 1–41.
Salvat, F., Salvat, B., 1992. Nukutipipi Atoll, Tuamotu Archipelago; geomorphology, land and marine flora and fauna and interrelationships. Atoll Res. Bull. 357, 1–43.
Schindelé, F., Hébert, H., Reymond, D., Sladen, A., 2006. L'aléa tsunami en Polynésie française: synthèse des observations et des mesures. Comptes Rendus Géoscience 338, 1133–1140.
Scicchitano, G., Pignatelli, C., Spampinato, C.R., Piscitelli, A., Milella, M., Monaco, C., Mastronuzzi, G., 2012. Terrestrial laser scanner techniques in the assessment of tsunami impact on the Maddalena peninsula (south-eastern Sicily, Italy). Earth Planets Space 64, 889–903.
Semah, F., 1979. Motu Tetaro (Raiatea). Premiers travaux archéologiques. Centre O.R.S.T.O.M. de Papeete, Direction des fouilles et antiquités..
Geographical Handbook Series, 1943. Pacific Islands, Volume II, Eastern Pacific. Naval Intelligence Division, London, p. 739.
Sinoto, Y.H., 1978. Preliminary report on the salvage excavation at Faahi'a Fare, Huahine Is., Society Islands, French Polynesia. Department of Anthropology, Bernice Panaki Bishop Museum, Honolulu, Hawaii..
Sladen, A., Hébert, H., Schindelé, F., Reymond, D., 2007. Evaluation of far-field tsunami hazard in French Polynesia based on historical data and numerical simulations. Nat. Hazards Earth Syst. Sci. 7, 195–206.
Southern Hemisphere Tropical Cyclone Data Portal, 2011. Pacific Climate Change Science Program. Bureau of Meteorology, Melbourne, Australia (Available at:) http://www.bom.gov.au/cyclone/history/tracks/.
Spiske, M., Böröcz, Z., Bahlburg, H., 2008. The role of porosity in discriminating between tsunami and hurricane emplacement of boulders—a case study from the lesser Antilles, southern Caribbean. Earth Planet. Sci. Lett. 268, 384–396.
Stephens, S.A., Ramsay, D.L., 2014. Extreme cyclone wave climate in the Southwest Pacific Ocean: influence of the El Niño southern oscillation and projected climate change. Glob. Planet. Chang. 123, 13–26.
Stine, S., 1990. Late Holocene fluctuations of mono Lake, Eastern California. Palaeogeogr. Palaeoclimatol. Palaeoecol. 78, 333–381.
Stoddart, D.R., 1969. Reconnaissance geomorphology of Rangiroa atoll, Tuamotu archipelago. Atoll Res. Bull. 125, 1–44.
Stoddart, D.R., Cann, J.R., 1965. Nature and origin of Beach Rock. J. Sediment. Petrol. 35 (1), 243–247.
Stoddart, D.R., Walsh, R.P.D., 1992. Enviornmental variability and environmental extremes as factors in the island ecosystem. Atoll Res. Bull. 356, 1–71.
Stone, G., 2015. Cyclone Pam Signals Slow-Motion Disaster in Kiribati. Conservation International Blog, Humanature (Available at:) http://blog.conservation.org/2015/03/cyclone-pam-signals-slow-motion-disaster-in-kiribati/.
Suzuki, A., Yokoyama, Y., Kan, H., Minoshima, K., Matsuzaki, H., Hamanaka, N., Kawahata, H., 2008. Identification of 1771 Meiwa tsunami deposits using a combination of radiocarbon dating and oxygen isotope microprofiling of emerged massive Porites boulders. Quat. Geochronol. 3, 226–234.
Tahitipress, 2010. Cyclone was French Polynesia's Worst in Decades. (Available at:) http://pidp.eastwestcenter.org/pireport/2010/February/02-15-04.htm.
Teissier, R., 1969. Les Cyclones en Polynésie Française (1878–1903–1905–1906) (Bulletin Societe Etudes Oceaniennes).
Terry, J.P., 2007. Tropical Cyclones: Climatology and Impacts in the South Pacific. Springer, New York.
Terry, J.P., Gienko, G., 2010. Climatological aspects of South Pacific tropical cyclones, based on analysis of the RSMC-Nadi (Fiji) regional archive. Clim. Res. 42 (3), 223–233.
Terry, J.P., Goff, J., 2014. Megaclasts: proposed revised nomenclature at the coarse end of the Udden-Wentworth grain-size scale for sedimentary particles. J. Sediment. Res. 84, 192–197.
Terry, J.P., Lau, A.Y.A., Etienne, S., 2013. Reef-Platform Coral Boulders: Evidence for High-Energy Marine Inundation Events on Tropical Coastlines. Springer, Singapore.
Toomey, M.R., Donnelly, J.P., Woodruff, J.D., 2013. Reconstructing mid-late Holocene cyclone variability in the Central Pacific using sedimentary records from Tahaa, French Polynesia. Quat. Sci. Rev. 77, 181–189.
Trichet, J., Repellin, P., Oustrière, P., 1984. Stratigraphy and subsidence of the Mururoa atoll (French Polynesia). Mar. Geol. 56, 241–257.
Vitousek, M.J., 1963. The tsunami of 22 may 1960 in French Polynesia. Bull. Seismol. Soc. Am. 53, 1229–1236.
Watt, S., Jaffe, B., Morton, R., Richmond, B., Gelfenbaum, G., 2010. Description of Extreme-Wave Deposits on the Northern Coast of Bonaire. U.S. Geological Survey Open-File Report 2010–1180, Netherlands Antille.
Wolter, K., Timlin, M.S., 2011. El Niño/southern oscillation behaviour since 1871 as diagnosed in an extended multivariate ENSO index (MEI.ext). Int. J. Climatol. 31, 1074–1087.
Yu, K., Zhao, J., Shi, Q., Meng, Q., 2009. Reconstruction of storm/tsunami records over the last 4000 years using transported coral blocks and lagoon sediments in the southern South China Sea. Quat. Int. 195, 128–137.
Yu, K., Zhao, J., Roff, G., Lybolt, M., Feng, Y., Clark, T., Li, S., 2012. High-precision U-series ages of transported coral blocks on heron reef (southern Great Barrier Reef) and storm activity during the past century. Palaeogeogr. Palaeoclimatol. Palaeoecol. 337-338, 23–36.
Zhao, J., Yu, K., Feng, Y., 2009. High-precision 238 U-234 U-230-Th disequilibrium dating of the recent past: a review. Quat. Geochronol. 4, 423–433.